

4-12-00

A

PATENT

Attorney Docket No. MASIMO.056DC1

Date: April 11, 2000

Page 1

ASSISTANT COMMISSIONER FOR PATENTS

WASHINGTON, D.C. 20231

ATTENTION: BOX PATENT APPLICATION

Sir:

Transmitted herewith for filing is the patent application of

Inventor(s): **Mohamed K. Diab and Rex J. McCarthy**For: **IMPROVED SIGNAL PROCESSING APPARATUS AND METHOD**

Enclosed are:

- (X) A specification in 43 pages.
- (X) Nineteen (19) sheets of drawings.
- (X) This application is a continuation of prior application 09/081,539 filed May 19, 1998, which is a divisional of application 08/834,194 filed April 14, 1997.
- (X) A copy of the Declaration from the parent application is enclosed.
- (X) Incorporation by Reference. The entire disclosure of the prior application, from which a copy of the oath or declaration is supplied is considered as being part of the disclosure of the accompanying application and is hereby incorporated by reference therein.
- (X) Please amend the specification by inserting the following sentence between the title and the section entitled Background of the Invention: "This application is a continuation of prior application 09/081,539 filed May 19, 1998 which is a divisional of application 08/834,194 filed April 14, 1997."
- (X) Please cancel claims 2-30.
- (X) Return prepaid postcard.

CLAIMS AS FILED

FOR	NUMBER FILED	NUMBER EXTRA	RATE	FEE
Basic Fee			\$690	\$690
Total Claims	1 - 20 =	0 x	\$18	\$0
Independent Claims	1 - 3 =	0 x	\$78	\$0

**FILING FEE TO BE PAID
AT A LATER DATE**

\$690

- (X) Please use Customer No. 20,995 for the correspondence address.

Lee W. Henderson
 Lee W. Henderson
 Registration No. 41,830
 Attorney of Record

H:\DOCS\LWHLWH-4204.DOC/b1 //041100

Knobbe, Martens, Olson & Bear, LLP
 620 Newport Center Dr. 16th Floor Newport Beach, CA 92660
 (949) 760-0404 FAX (949) 760-9502

jc586 U.S. PTO
 04/11/00

jc525 U.S. PTO

09/54/588

04/11/00

09547588 041100

KNOBBE, MARTENS, OLSON & BEARA LIMITED LIABILITY PARTNERSHIP INCLUDING
PROFESSIONAL CORPORATIONS

PATENT, TRADEMARK AND COPYRIGHT CAUSES

620 NEWPORT CENTER DRIVE

SIXTEENTH FLOOR

NEWPORT BEACH, CALIFORNIA 92660-8016

(949) 760-0404

FAX (949) 760-9502

INTERNET: WWW.KNOB.COM

LOUIS J. KNOBBE*
DON W. MARTENS*
GORDON H. OLSON*
JAMES B. BEAR
DARRELL L. OLSON*
WILLIAM B. BUNKER
WILLIAM H. NIEMAN
ARTHUR S. ROSE
JAMES F. LESNIAK
NED A. ISRAELSEN
DREW S. HAMILTON
JERRY T. SEWELL
JOHN B. SGANGA, JR.
EDWARD A. SCHLATTER
GERARD VON HOFFMANN
JOSEPH R. RE
CATHERINE J. HOLLAND
JOHN M. CARSON
KAREN VOGEL WEIL
ANDREW H. SIMPSON
JEFFREY L. VAN HOESEAR
DANIEL E. ALTMAN
MARGUERITE L. GUNN
STEPHEN C. JENSEN
VITO A. CANUSO III
WILLIAM H. SHREVE
LYNDA J. ZADRA-SYMES†
STEVEN J. NATAUPSKY
PAUL A. STEWART
JOSEPH F. JENNINGS
CRAIG S. SUMMERS
ANNEMARIE KAISER
BRENTON R. BABCOCK

THOMAS F. SMEGAL, JR.
MICHAEL H. TRENHOLM
DIANE M. REED
JONATHAN A. BARNEY
RONALD J. SCHOENBAUM
JOHN R. KING
FREDERICK S. BERRETTA
NANCY WAYS VENSKO
JOHN P. GIEZENTANNER
ADEEL S. AKHTAR
GINGER R. DREGER
THOMAS R. ARNO
DAVID N. WEISS
DANIEL HART, PH.D.
DOUGLAS G. MUEHLHAUSER
LORI LEE YAMATO
MICHAEL K. FRIEDLAND
STEPHEN M. LOBBIN
STACEY R. HALPERN
DALE C. HUNT, PH.D.
LEE W. HENDERSON, PH.D.
DEBORAH S. SHEPHERD
RICHARD E. CAMPBELL
MARK M. ABUMERI
JON W. GURKA
ERIC M. NELSON
ALEXANDER C. CHEN
MARK R. BENEDICT, PH.D.
PAUL N. CONOVER
ROBERT J. ROBY
SABING H. LEE
KAROLINE A. DELANEY
JOHN W. HOLCOMB

JAMES J. MULLEN, III, PH.D.
JOSEPH S. CIANFRANI
JOSEPH M. REISMAN, PH.D.
WILLIAM R. ZIMMERMAN
GLEN L. NUTTALL
ERIC S. FURMAN, PH.D.
TIRZAH ABE LOWE
GEOFFREY Y. IIDA
ALEXANDER S. FRANCO
SANJIVPAL S. GILL
SUSAN M. MOSS
JAMES W. HILL, M.D.
ROSE M. THIessen, PH.D.
MICHAEL L. FULLER
MICHAEL A. GUILIANA
MARK J. KERTZ
RABINDER N. NARULA
BRUCE S. ITCHKAWITZ, PH.D.
PETER M. MIDGLEY
THOMAS S. MCCLENAHAN
MICHAEL S. OKAMOTO
JOHN M. GROVER
MALLARY K. DE MERLIER
IRFAN A. LATEEF
AMY C. CHRISTENSEN
SHARON S. NG
MARK J. GALLAGHER, PH.D.
DAVID G. JANKOWSKI, PH.D.
BRIAN C. HORNE
PAYSON J. LEMEILLEUR
WILLIAM G. BERRY

OF COUNSEL
JERRY R. SEILER
JAPANESE PATENT ATTY
KATSUHIRO ARAI**

EUROPEAN PATENT ATTY
MARTIN HELLEBRANDT

KOREAN PATENT ATTY
MINCHEOL KIM

SCIENTISTS & ENGINEERS
(NON-LAWYERS)

RAIMOND J. SALENIEKS**
NEIL S. BARTFELD, PH.D.**
DANIEL E. JOHNSON, PH.D.**
JEFFERY KOEPKE, PH.D.
KHURRAM RAHMAN, PH.D.
JENNIFER A. HAYNES, PH.D.
BRENDAN P. O'NEILL, PH.D.
THOMAS Y. NAGATA
ALAN C. GORDON
LINDA H. LIU
YASHWANT VAISHNAV, PH.D.
MEGUMI TANAKA
ANDREW N. MERICKEL
CHE S. CHERESKIN, PH.D.**
JASON I. SAATHOFF
ERIK W. ARCHBOLD
PHILIP C. HARTSTEIN
JULIE A. HOPPER
CHRIS S. CASTLE

* A PROFESSIONAL CORPORATION
† ALSO BARRISTER AT LAW (U.K.)
** U.S. PATENT AGENT

Assistant Commissioner for Patents
Washington, D.C. 20231

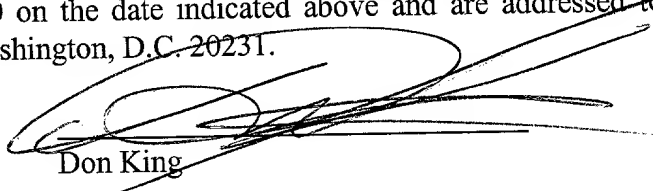
CERTIFICATE OF MAILING BY "EXPRESS MAIL"

Attorney Docket No. : MASIMO.056DC1
Applicant(s) : Mohamed K. Diab and Rex J. McCarthy
For : IMPROVED SIGNAL PROCESSING
APPARATUS AND METHOD
Attorney : Lee W. Henderson
"Express Mail"
Mailing Label No. : EL 523 238 812 US
Date of Deposit : April 11, 2000

I hereby certify that the accompanying

Transmittal in Duplicate; Specification in 43 pages; 19 sheets of drawings; Copy
of Declaration by Inventor; Return Prepaid Postcard

are being deposited with the United States Postal Service "Express Mail Post Office to
Addressee" service under 37 CFR 1.10 on the date indicated above and are addressed to the
Assistant Commissioner for Patents, Washington, D.C. 20231.


Don King

H:\DOCS\LWH\LWH-4205.DOC
041100

201 CALIFORNIA STREET
SUITE 1150
SAN FRANCISCO, CALIFORNIA 94111
(415) 954-4114
FAX (415) 954-4111

501 WEST BROADWAY
SUITE 1400
SAN DIEGO, CALIFORNIA 92101
(619) 235-8550
FAX (619) 235-0176

3801 UNIVERSITY AVENUE
SUITE 710
RIVERSIDE, CALIFORNIA 92501
(909) 781-9231
FAX (909) 781-4507

1875 CENTURY PARK EAST
SUITE 600
LOS ANGELES, CALIFORNIA 90067
(310) 407-5484
FAX (310) 407-5485

IMPROVED SIGNAL PROCESSING APPARATUS AND METHODBackground of the InventionField of the Invention

5 The present invention relates to the field of signal processing. More specifically, the present invention relates to the processing of measured signals, containing a primary signal portion and a secondary signal portion, for the removal or derivation of either the primary or secondary signal portion when little is known about either of these components. The present invention is especially useful for physiological monitoring systems including blood oxygen saturation systems and
10 pulserate measurement systems. The present invention further relates to a method and apparatus for signal processing of signals in order to compute an estimate for pulserate.

Description of the Related Art

15 Signal processors are typically employed to remove or derive either the primary or secondary signal portion from a composite measured signal including a primary signal portion and a secondary signal portion. For example, a composite signal may contain a primary signal portion comprising desirable data and a secondary signal portion comprising noise. If the secondary signal portion occupies a different frequency spectrum than the primary signal portion, then conventional filtering
20 techniques such as low pass, band pass, and high pass filtering are available to remove or derive either the primary or the secondary signal portion from the total signal. Fixed single or multiple notch filters could also be employed if at least one of the primary and secondary signal portions exists at a fixed frequency band.

25 It is often the case that an overlap in frequency spectrum between the primary and secondary signal portions exists. Complicating matters further, the statistical properties of one or both of the primary and secondary signal portions may change with time. In such cases, conventional filtering techniques are ineffective in extracting either the primary or secondary signal. If, however, a description of either the primary or secondary signal portion can be derived, correlation canceling, such as adaptive
30 noise canceling, can be employed to remove either the primary or secondary signal

portion of the signal isolating the other portion. In other words, given sufficient information about one of the signal portions, that signal portion can be extracted.

Conventional correlation cancelers, such as adaptive noise cancelers, dynamically change their transfer function to adapt to and remove portions of a composite signal. However, correlation cancelers and adaptive noise cancelers require either a secondary reference or a primary reference which correlates to either the secondary signal portion only or the primary signal portion only. For instance, for a measured signal containing noise and desirable signal, the noise can be removed with a correlation canceler if a noise reference is available. This is often the case. Although the amplitudes of the reference signals are not necessarily the same as the amplitudes of the corresponding primary or secondary signal portions, the reference signals have a frequency spectrum which is similar to that of the primary or secondary signal portions.

In many cases, nothing or very little is known about the secondary and primary signal portions. One area where measured signals comprising a primary signal portion and a secondary signal portion about which no information can easily be determined is physiological monitoring. Physiological monitoring generally involves measured signals derived from a physiological system, such as the human body. Measurements which are typically taken with physiological monitoring systems include electrocardiographs, blood pressure, blood gas saturation (such as oxygen saturation), capnographs, other blood constituent monitoring, heart rate, respiration rate, electro-encephalograph (EEG) and depth of anesthesia, for example. Other types of measurements include those which measure the pressure and quantity of a substance within the body such as cardiac output, venous oxygen saturation, arterial oxygen saturation, bilirubin, total hemoglobin, breathalyzer testing, drug testing, cholesterol testing, glucose testing, and carbon dioxide testing, protein testing, carbon monoxide testing, and other in-vivo measurements, for example. Complications arising in these measurements are often due to motion of the patient, both external and internal (muscle movement, vessel movement, and probe movement, for example), during the measurement process.

Many types of physiological measurements can be made by using the known properties of energy attenuation as a selected form of energy passes through a test medium such as a finger, shown schematically in Figure 1.

A blood gas monitor is one example of a physiological monitoring system which is based upon the measurement of energy attenuated by biological tissues or substances. Blood gas monitors transmit light into the test medium and measure the attenuation of the light as a function of time. The output signal of a blood gas monitor which is sensitive to the arterial blood flow contains a component having a waveform representative of the patient's arterial pulse. This type of signal, which contains a component related to the patient's pulse, is called a plethysmographic wave, and is shown in Figure 2A as a curve $s(t)$ 201. Plethysmographic waveforms are used in blood gas saturation measurements. As the heart beats, the amount of blood in the arteries increases and decreases, causing increases and decreases in energy attenuation, illustrated by a cyclic wave seen in the curve 201.

Typically, a digit such as a finger, an ear lobe, or other portion of the body where blood flows close to the skin, is employed as the medium through which light energy is transmitted for blood gas attenuation measurements. The finger comprises skin, fat, bone, muscle, etc., as shown Figure 1, each of which attenuates energy incident on the finger in a generally predictable and constant manner. However, when fleshy portions of the finger are compressed erratically, for example by motion of the finger, energy attenuation becomes erratic.

An example of a more realistic measured waveform is shown in Figure 2B, as a curve $M(t)$ 202. The curve 202 illustrates the effect of motion and noise $n(t)$ added to the clean waveform $s(t)$ shown in figure 201. The primary plethysmographic waveform portion of the signal $M(t)$ is the waveform representative of the pulse, corresponding to the sawtooth-like pattern wave in curve 201. The large, secondary motion-induced excursions in signal amplitude obscure the primary plethysmographic signal $s(t)$. Even small variations in amplitude make it difficult to distinguish the primary signal component $s(t)$ in the presence of a secondary signal component $n(t)$.

A pulse oximeter is a type of blood gas monitor which non-invasively measures the arterial saturation of oxygen in the blood. The pumping of the heart

forces freshly oxygenated blood into the arteries causing greater energy attenuation. As well understood in the art, the arterial saturation of oxygenated blood may be determined from the depth of the valleys relative to the peaks of two plethysmographic waveforms measured at separate wavelengths. Patient movement introduces motion artifacts to the composite signal as illustrated in the plethysmographic waveform illustrated in Figure 2B. These motion artifacts distort the measured signal.

Summary of the Invention

The present invention involves several different embodiments using the novel signal model in accordance with the present invention to estimate the desired signal portion of a measured data signal where the measured data contains desired and undesired components. In one embodiment, a signal processor acquires a first measured signal and a second measured signal. The first signal comprises a desired signal portion and an undesired signal portion. The second measured signal comprises a desired signal portion and an undesired signal portion. The signals may be acquired by propagating energy through a medium and measuring an attenuated signal after transmission or reflection. Alternatively, the signals may be acquired by measuring energy generated by the medium.

In one embodiment, the desired signal portions of the first and second measured signals are approximately equal to one another, to within a first constant multiplier. The undesired signal portions of the first and second measured signals are also approximately equal to one another, to within a second constant multiplier. A scrubber coefficient may be determined, such that an estimate for the first signal can be generated by inputting the first and second measured signals, and the scrubber coefficient into a waveform scrubber. The output of the waveform scrubber is generated by multiplying the first measured signal by the scrubber coefficient and then adding the result to the second measured signal.

In one embodiment, the scrubber coefficient is determined by normalizing the first and second measured signals, and then transforming the normalized signals into a spectral domain. The spectral domain signals are then divided by one another to produce a series of spectral ratio lines. The need for waveform scrubbing can be

00140 884560

determined by comparing the largest ratio line to the smallest ratio line. If the difference does not exceed a threshold value, the no scrubbing is needed. If the difference does exceed a threshold value, then the waveform must be scrubbed, and the scrubbing coefficient corresponds to the magnitude of the largest ratio line.

5 Another aspect of the present invention involves a physiological monitor having a signal processor which computes an estimate for an unknown pulserate from the measured data. In one embodiment, the signal processor receives measured data from a detector that measures a physiological property related to the heartbeat. The signal processor transforms the data into a spectral domain and then identifies a series
10 of spectral peaks and the frequencies associated with those peaks. The signal processor then applies a set of rules to the spectral peaks and the associated frequencies in order to compute an estimate for the pulserate.

In yet another embodiment of the pulserate detector, the signal processor performs a first transform to transform the measured data into a first transform space.
15 The signal processor then performs a second transform to transform the data from the first transform space into a second transform space. The signal processor then searches the data in the second transform space to find the pulserate.

In another embodiment, the transform into the first transform space is a spectral transform such as a Fourier transform. In another embodiment, the transform into the
20 second transform space is a spectral transform such as a Fourier transform. In yet another embodiment, once the data has been transformed into the second transform space, the signal processor performs a $1/x$ mapping on the spectral coordinates before searching for the pulserate.

In another embodiment, the signal processor transforms the measured data into
25 a first spectral domain, and then transforms the data from the first spectral domain into a second spectral domain. After twice transforming the data, the signal processor performs a $1/x$ remapping on the coordinates of the second spectral domain. The signal processor then searches the remapped data for the largest spectral peak corresponding to a pulserate less than 120 beats per minute. If such a peak is found,
30 then the signal processor outputs the frequency corresponding to that peak as being the pulserate. Otherwise, the signal processor searches the data transformed into the

first spectral domain for the largest spectral peak in that domain, and outputs a pulserate corresponding to the frequency of the largest peak in the first spectral domain.

5 In another embodiment of the pulserate detector, the signal processor first transforms the measured data into a first spectral domain. Then the signal processor takes the magnitude of the transformed data and then transforms the magnitudes into a second spectral domain. Then the signal processor then performs a $1/x$ mapping of the spectral coordinates. After the $1/x$ mapping, the signal processor feeds the transformed and remapped data into a neural network. The output of the neural
10 network is the pulserate.

Brief Description of the Drawings

Figure 1 schematically illustrates a typical finger.

Figure 2A illustrates an ideal plethysmographic waveform.

15 Figure 2B illustrates a plethysmographic waveform which includes a motion-induced erratic signal portion.

Figure 3 illustrates a schematic diagram of a physiological monitor in accordance with the teachings of one aspect of the present invention

20 Figure 4 illustrates an example of a low noise emitter current driver with accompanying digital to analog converter in accordance with the teachings of one aspect of the present invention.

Figure 5 illustrates the absorption properties of hemoglobin at various wavelength.

Figure 6 illustrates one cycle of an idealized plethysmographic waveform for various levels of oxygen saturation at a fixed perfusion.

25 Figure 7 illustrates a block diagram of the signal processing used to compute the ratio of red signal to infrared signal in accordance with one aspect of the present invention.

Figure 8 is a graph which illustrates the relationship between the red/infrared ratio and blood oxygen saturation.

30 Figure 9 is a graph which illustrates the relationship between the ideal red and infrared signals, and the relationship between measured red and infrared signals.

Figure 10 illustrates a model for measured data in a pulse oximeter.

Figure 11 is an idealized frequency domain plot of the red and infrared transmission signals

5 Figure 12 is a block diagram of a motion detector and removal system in accordance with one aspect of the present invention.

Figure 13 is a flowchart showing the processing steps of a motion detector and removal method in accordance with one aspect of the present invention.

Figure 14A is an idealized frequency domain plot of an plethysmographic wave.

10 Figure 14B is an idealized frequency domain plot of a plethysmographic wave showing the effect of FM modulation.

Figure 14C is an idealized time domain plot of a superimposed pair of plethysmographic waves that can be used to model an FM modulated plethysmographic wave.

15 Figure 15 is an idealized frequency domain plot of a plethysmographic wave showing the effects of AM modulation.

Figure 16 is a group of idealized frequency domain plots that illustrate the various categories used in the rule based method for determining pulserate in accordance with one aspect of the present invention.

20 Figure 17 is a block diagram which illustrates the signal processing used to determine pulse rate by the pleth to pulserate transform method (PPRT) in accordance with one aspect of the present invention.

Figure 18 is a flowchart showing the process steps of the rule based pulserate detection method.

25 Figure 19 illustrates a schematic diagram of a physiological monitor that uses a neural network in accordance with the teachings of one aspect of the present invention.

Detailed Description of the Invention

30 The present invention involves a system which uses first and second measured signals that each contain a primary signal portion and a secondary signal portion. In other words, given first and second composite signals $c_1(t) = s_1(t) + n_1(t)$ and

09547588-04100

$c_2(t) = s_2(t) + n_2(t)$, the system of the present invention can be used to isolate either the primary signal portion $s(t)$ or the secondary signal portion $n(t)$ of the two composite signals. Following processing, the output of the system provides a good approximation $n''(t)$ to the secondary signal portion $n(t)$ or a good approximation $s''(t)$ to the primary signal portion $s(t)$.

The system of the present invention is particularly useful where the primary signal portion $s(t)$, the secondary signal portion $n(t)$, or both, may contain one or more of a constant portion, a predictable portion, an erratic portion, a random portion, etc. The primary signal approximation $s''(t)$ or the secondary signal approximation $n''(t)$ is derived by removing as many of the secondary signal portions $n(t)$ or primary signal portions $s(t)$ from the composite signal $c(t)$ as possible. The remaining signal forms either the primary signal approximation $s''(t)$ or the secondary signal approximation $n''(t)$, respectively. The constant portion and the predictable portion of the secondary signal $n(t)$ are easily removed with traditional filtering techniques, such as simple subtraction, low pass, band pass, and high pass filtering. The erratic portion is more difficult to remove due to its unpredictable nature. If something is known about the erratic signal, even statistically, it could be removed, at least partially, from the measured signal via traditional filtering techniques. However, often no information is known about the erratic portion of the secondary signal $n(t)$. In this case, traditional filtering techniques are usually insufficient.

In order to remove the secondary signal $n(t)$, a signal model in accordance with the present invention is defined as follows for the first and second measured signals c_1 and c_2 :

$$c_1 = s_1 + n_1 \quad (1)$$

$$c_2 = s_2 + n_2 \quad (2)$$

$$\text{with } s_1 = r_a s_2 \text{ and } n_1 = r_v n_2 \quad (3)$$

$$\text{or} \quad r_a = \frac{s_1}{s_2} \quad \text{and} \quad r_v = \frac{n_1}{n_2} \quad (4)$$

where s_1 and n_1 are at least somewhat (preferably substantially) uncorrelated and s_2 and n_2 are at least somewhat (preferably substantially) uncorrelated. The first and second measured signals c_1 and c_2 are related by correlation coefficients r_a and r_v as defined above. The use and selection of these coefficients is described in further detail below.

In accordance with one aspect of the present invention, this signal model is used in combination with a waveform scrubber to remove the undesired portion of the measured signals.

The description that follows can best be understood in view of the following list which briefly describes how the invention is broken down and described according to the following topics:

1. A general overview of pulse oximetry measurements, in connection with Figures 1 through 4, provides a general theory and system block diagram for a red/infrared pulse oximetry apparatus for measurement of physiological data such as blood oxygen saturation and pulserate;

2. A more detailed description of the relationship between the data $RD(t)$ measured using red light, and the data $IR(t)$ measured using infrared light, normalization of $RD(t)$ and $IR(t)$, and the relationship of the normalized $RD(t)$ and $IR(t)$ to blood oxygen saturation, is provided in connection with Figures 5 through 8;

3. A mathematical model and description of the effect of motion artifacts on $RD(t)$ and $IR(t)$ and a method for detecting and removing the artifacts to create a clean spectrum $F(\omega)=RD(\omega)/IR(\omega)$, are provided in connection with Figures 10 through 13;

4. A mathematical model and a description of a rule based signal processing technique used by the pulse oximeter to determine pulserate, are provided in connection with Figures 14 through 16; and

5. A mathematical model and a description of a transform based signal processing technique used by the pulse oximeter to determine pulserate, are provided in connection with Figure 17.

PULSE OXIMETRY MEASUREMENTS

5 A specific example of a physiological monitor using a processor of the present invention to determine a secondary reference $n'(t)$ for input to a canceler that removes erratic motion-induced secondary signal portions is a pulse oximeter. Pulse oximetry may also be performed using a processor of the present invention to determine a primary signal reference $s'(t)$ which may be used for display purposes or for input to
10 a processor to derive information about patient movement, pulserate, and venous blood oxygen saturation.

A pulse oximeter typically causes energy to propagate through a medium where blood flows close to the surface, for example, an ear lobe, or a digit such as a finger, a forehead or a fetus' scalp. An attenuated signal is measured after propagation
15 through or reflected from the medium. The pulse oximeter estimates the saturation of oxygenated blood.

Freshly oxygenated blood is pumped at high pressure from the heart into the arteries for use by the body. The volume of blood in the arteries and arterioles varies with the heartbeat, giving rise to a variation in absorption of energy at the rate of the heartbeat, or the pulse. The blood scatters both red and infrared light, and thus as the
20 volume of blood changes, the amount of scattering changes as well. Typically the effects due to scattering are small when compared to the effects due to the change in blood volume.

Oxygen depleted, or deoxygenated, blood is returned to the heart by the veins along with unused oxygenated blood. The volume of blood in the veins varies with
25 back pressure due to breathing as well as local uncontrolled motion of muscles. These variations typically occur at a rate that is much slower than the heartbeat. Thus, when there is no motion induced variation in the thickness of the veins, venous blood causes a low frequency variation in absorption of energy. When there is motion induced variation in the thickness of the veins, the scattering changes as well and this
30 absorption is coupled with the erratic variation in absorption due to motion artifacts.

00147588-04100

In absorption measurements using the transmission of energy through a medium, two light emitting diodes (LEDs) are positioned close to a portion of the body where blood flows close to the surface, such as a finger, and a photodetector is positioned near the LEDs. Typically, in pulse oximetry measurements, one LED emits a visible wavelength, preferably red, and the other LED emits an infrared wavelength. However, one skilled in the art will realize that other wavelength combinations, as well as combinations of more than two wavelengths, could be used. The finger comprises skin, tissue, muscle, both arterial blood and venous blood, fat, etc., each of which absorbs light energy differently due to different absorption coefficients, different concentrations, different thicknesses, and changing optical pathlengths. When the patient is not moving, absorption is substantially constant except for the flow of blood. The constant attenuation can be determined and subtracted from the signal via traditional filtering techniques. When the patient moves, this causes perturbation such as changing optical pathlength due to movement of background fluids (e.g., venous blood having a different saturation than the arterial blood). Therefore, the measured signal becomes erratic. Erratic motion induced noise typically cannot be predetermined and/or subtracted from the measured signal via traditional filtering techniques. Thus, determining the oxygen saturation of arterial blood and venous blood becomes more difficult.

Figure 3 depicts a general hardware block diagram of a pulse oximeter 299. A sensor 300 has two light emitters 301 and 302, such as LED's. One LED 301 emitting light of red wavelengths and another LED 302 emitting light of infrared wavelengths are placed adjacent a finger 310. A photodetector 320, which produces an electrical signal corresponding to the attenuated visible and infrared light energy signals is, located near the LED's 301 and 302. The photodetector 320 is connected to front end analog signal conditioning circuitry 330.

The front end analog signal conditioning circuit 330 has outputs coupled to an analog to digital conversion circuit 332. The analog to digital conversion circuit 332 has outputs coupled to a digital signal processing system 334. The digital signal processing system 334 provides the desired parameters as outputs for a display 336.

Outputs for display are, for example, blood oxygen saturation, heart rate, and a clean plethysmographic waveform.

The signal processing system also provides an emitter current control output 337 to a digital-to-analog converter circuit 338 which provides control information for a set of light emitter drivers 340. The light emitter drivers 340 couple to the light emitters 301, 302. The digital signal processing system 334 also provides a gain control output 343 for the front end analog signal conditioning circuitry 330.

Figure 4 illustrates a preferred embodiment for the combination of the emitter drivers 340 and the digital to analog conversion circuit 338. As depicted in Figure 4, the driver comprises first and second input latches 321, 322, a synchronizing latch 323, a voltage reference 324, a digital to analog conversion circuit 325, first and second switch banks 326, 327, first and second voltage to current converters 328, 329 and the LED emitters 301, 302 corresponding to the LED emitters 301, 302 of Figure 3.

The preferred driver depicted in Figure 4 is advantageous in that the present inventors recognized that much of the noise in the oximeter 299 of Figure 3 is caused by the LED emitters 301, 302. Therefore, the emitter driver circuit of Figure 4 is designed to minimize the noise from the emitters 301, 302. The first and second input latches 321, 322 are connected directly to the digital signal processor (DSP) bus 337. Therefore, the action of these latches significantly minimizes the bandwidth (resulting in noise) present on the DSP bus 337 which passes through to the driver circuitry of Figure 4. The outputs of the first and second input latches 321, 322, only change when the latches detect their respective address on the DSP bus 337. The first input latch 321, receives the setting for the digital to analog converter circuit 325. The second input latch 322 receives switching control data for the switch banks 326, 327. The synchronizing latch 323 accepts the synchronizing pulses which maintain synchronization between the activation of emitters 301, 302 and the analog to digital conversion circuit 332.

The voltage reference 324 is also chosen as a low noise DC voltage reference for the digital to analog conversion circuit 325. In addition, in the present embodiment, the voltage reference 324 has a lowpass output filter with a very low

corner frequency (e.g., 1 Hz in the present embodiment). The digital to analog converter 325 also has a lowpass filter at its output with a very low corner frequency (e.g., 1 Hz). The digital to analog converter 338 provides signals for each of the emitters 301, 302.

5 In the present embodiment, the output of the voltage to current converters 328, 329 are switched such that with the emitters 301, 302 connected in back-to-back configuration, only one emitter is active an any given time. In addition, the voltage to current converter 328 or 329 for the inactive emitter is switched off at its input as well, such that it is completely deactivated. This reduces noise from the switching and
10 voltage to current conversion circuitry. In the present embodiment, low noise voltage to current converters are selected (e.g., Op 27 Op Amps), and the feedback loop is configured to have a low pass filter to reduce noise. In the present embodiment, the low pass filtering function of the voltage to current converters 328, 329 has a corner frequency of just above 316.7 Hz, which is the switching speed for the emitters, as
15 further discussed below. Accordingly, the preferred driver circuit of Figure 4, minimizes the noise of the emitters 301, 302.

In general, each of the red and infrared light emitters 301, 302 emits energy which is partially absorbed by the finger 310 and the remaining energy is received by the photodetector 320. The photodetector 320 produces an electrical signal which
20 corresponds to the intensity of the light energy striking the photodetector 320. The front end analog signal conditioning circuitry 330 receives the intensity signals and filters and conditions these signals, as further described below, for further processing. The resultant signals are provided to the analog-to-digital conversion circuitry 332 which converts the analog signals to digital signals for further processing by the
25 digital signal processing system 334. In the present embodiment, the output of the digital signal processing system 334 provides clean plethysmographic waveforms of the detected signals and provides values for oxygen saturation and pulse rate to the display 336.

It should be understood that in different embodiments of the present invention,
30 one or more of the outputs may be provided. The digital signal processing system 334 also provides control for driving the light emitters 301, 302 with an emitter current

control signal on the emitter current control output 337. This value is a digital value which is converted by the digital-to-analog conversion circuit 338 which provides a control signal to the emitter current drivers 340. The emitter current drivers 340 provide the appropriate current drives for the red emitter 301 and the infrared emitter 302. Further detail of the operation of the physiological monitor for pulse oximetry is explained below.

In the present embodiment, the light emitters 301, 302 are driven via the emitter current driver 340 to provide light transmission with digital modulation at 316.7 Hz. In the present embodiment, the light emitters 301, 302 are driven at a power level which provides an acceptable intensity for detection by the detector and for conditioning by the front end analog signal conditioning circuitry 330. Once this energy level is determined for a given patient by the digital signal processing system 334, the current level for the red and infrared emitters is maintained constant. It should be understood, however, that the current may be adjusted for changes in the ambient room light and other changes which would effect the voltage input to the front end analog signal conditioning circuitry 330. In the present invention, the red and infrared light emitters 301, 302 are modulated as follows: for one complete 316.7 Hz red cycle, the red emitter 301 is activated for the first quarter cycle, and off for the remaining three-quarters cycle; for one complete 316.7 Hz infrared cycle, the infrared light emitter 302 is activated for one quarter cycle and is off for the remaining three-quarters cycle. In order to only receive one signal at a time, the emitters are cycled on and off alternatively, in sequence, with each only active for a quarter cycle per 316.7 Hz cycle and with a quarter cycle separating the active times.

The light signal is attenuated (amplitude modulated) by the pumping of blood through the finger 310 (or other sample medium). The attenuated (amplitude modulated) signal is detected by the photodetector 320 at the 316.7 Hz carrier frequency for the red and infrared light. Because only a single photodetector is used, the photodetector 320 receives both the red and infrared signals to form a time division multiplexed (TDM) signal. The TDM signal is provided to the front analog signal conditioning circuitry 330 and may be demodulated by either before or after analog to digital conversion.

Saturation Curves and Normalization

The ability of the apparatus 299 to measure the desired physiologic properties lies in the optical absorption properties of hemoglobin, as illustrated in Figure 5. Figure 5 shows an x axis 501 corresponding to a wavelength of light and a y axis 502 corresponding to an absorption coefficient for light passing through a medium. A reduced hemoglobin (Hb) curve 503 shows the absorption properties of oxygen poor hemoglobin. An oxygen rich hemoglobin (HbO2) curve 504 shows the absorption properties of oxygen rich hemoglobin. A reference line 506 highlights the region where the curves 503 and 504 pass through a value on the x axis 501 corresponding to 660 nm (nanometer) wavelength (the nominal operational wavelength of the red emitter 301). A reference line 505 highlights the region where the curves 503 and 504 pass through a value on the x axis 501 corresponding to 905 nm wavelength (the nominal operational wavelength of the infrared emitter 302).

At the reference line 506, the Hb curve 503 shows more absorption than the HbO2 curve 504. Conversely, at the reference line 505, the HbO2 curve shows more absorption than the Hb curve 503. The pulse oximeter can thus measure the blood oxygen saturation by measuring absorption of the blood at 660 nm and 905 nm, and the comparing the two absorption measurements.

According to the Beer-Lambert law of absorption, the intensity of light transmitted through an absorbing medium is given by:

$$I = I_0 e^{-\epsilon dc} \quad (5)$$

where I_0 is the intensity of the incident light, ϵ is the absorption coefficient, c is the concentration coefficient and d is the thickness of the absorbing medium. In pulse oximetry applications, there are two sources, red and infrared, and thus two incident intensities, $I_{0,RD}$ for red, and $I_{0,IR}$ for infrared. Furthermore, in blood there are two concentrations of interest, namely the concentration of oxygen poor hemoglobin, denoted by C_{Hb} and the concentration of oxygen rich hemoglobin, denoted by C_{HbO_2} . The combination of the two optical wavelengths and the two concentrations means that there are four absorption coefficients, namely $\epsilon_{RD,Hb}$, ϵ_{RD,HbO_2} , $\epsilon_{IR,Hb}$, and ϵ_{IR,HbO_2} .

Using these quantities, and assuming no time variation in any of the values except d , gives two separate Beer-Lambert equations for the pulse oximeter.

$$I_{RD} = I_{0, RD} e^{-[\epsilon_{RD, Hb} C_{Hb} + \epsilon_{RD, HbO_2} C_{HbO_2}] d(t)} \quad (6)$$

$$I_{IR} = I_{0, IR} e^{-[\epsilon_{IR, Hb} C_{Hb} + \epsilon_{IR, HbO_2} C_{HbO_2}] d(t)} \quad (7)$$

The measurement apparatus 299 does not provide a capability for measuring the incident terms $I_{0, RD}$ and $I_{0, IR}$ appearing in the above equation, and thus, strictly speaking, the value of I_{RD} and I_{IR} cannot be determined. However, in the pulse oximeter, only differential measurements are necessary. In other words, it is only the time varying nature of the values I_{RD} and I_{IR} and the relationship between the values that are important. The time variation in $d(t)$ occurs primarily because blood flows in and out of the finger with each heartbeat. As blood flows into the finger, the effective value of d , as well as the scattering component, increases, and as blood flows out, the effective value of d and the scattering decreases. There are also time variations in the concentrations C_{Hb} and C_{HbO_2} as the blood oxygen saturation level changes. Fortunately, these variations are slow compared to the variations in $d(t)$, and they can be ignored.

Figure 6 illustrates one cycle of an idealized plethysmographic waveform for various levels of oxygen saturation. The figure shows an x-y plot having a time axis 601 in the x direction, and a transmission axis 602 in the y direction. The transmission axis 602 shows the intensity of the red light transmitted through the finger. A curve 604 shows the transmission of red light for 80% blood oxygen saturation. A curve 603 shows transmission of red light for 98% blood oxygen saturation. The curves 603 and 604 are intended to show different values of saturation given the same perfusion d . As shown in the figure, at the beginning of a heartbeat, red transmission is at a maximum because the finger contains relatively little blood. As the heartbeat progresses, blood is perfused into the finger and the amount of light transmission diminishes. Transmission diminishes because the additional material, the blood, increases the effective path length d in Equation (6). Transmission also diminishes somewhat because of scattering produced by the blood. If the blood is

highly saturated with oxygen, as shown in the curve 603, the transmission diminishes only slightly because, as shown in Figure 5, HbO₂ has a relatively small absorption coefficient in the red wavelengths. If the blood has low oxygen saturation, as shown in the curve 604, then transmission diminishes significantly more because, as shown in Figure 5, Hb has a relatively large absorption in the red wavelengths.

If Figure 6 were redrawn to show the transmission properties of infrared light, then the curves 603 and 604 would essentially be interchanged, because as shown in Figure 5, more infrared light is absorbed by HbO₂ than is absorbed by Hb.

The above properties of the absorption of light by Hb and HbO₂ advantageously provide a way to measure blood oxygen saturation by computing the ratio of red light to infrared light. Figure 7 shows one embodiment of a signal processing apparatus for obtaining the desired ratio. Figure 7 shows a red signal path which begins at a RD signal input 701. The RD signal input 701 corresponds to the amount of red light transmitted through the finger. The signal at the RD signal input 701 is fed into a logarithmic amplifier 702 which in turn feeds a bandpass filter 703. The output of the bandpass filter 703 is fed into a root-means-square (RMS) detector 704. The output of the RMS detector 704 is fed to a numerator input of a divider 709. Figure 7 further shows an IR signal path comprising an IR input 705, a logarithmic amplifier 706, a bandpass filter 707, and an RMS detector 708. The output of the RMS detector 708 is fed to a denominator input of the divider 709.

In a preferred embodiment, the elements shown in Figure 7 are part of the signal processing block 334 shown in Figure 3. The RD input 701 and IR input 705 are obtained by demultiplexing the output of the detector 320, also shown in Figure 3. The signals at the inputs 701 and 705 correspond to I_{RD} and I_{IR} respectively, and are similar to the curves shown in Figure 6. However, in the preferred embodiment, the signals are uncalibrated (i.e., the scale of the y axis 602 is unknown) because the value of $I_{0, RD}$ and $I_{0, IR}$ in Equations (6) and (7) are unknown. This is not an impediment to the measurement of the blood oxygen saturation, because saturation can be obtained without reference to either $I_{0, RD}$ or $I_{0, IR}$ as follows. Taking the natural logarithm (in signal processing blocks 702 and 706) of both Equation (6) and Equation (7) yields:

$$\ln(I_{RD}) = \ln(I_{0,RD}) - [\epsilon_{RD,Hb} C_{Hb} + \epsilon_{RD,HbO2} C_{HbO2}] d(t) \quad (8)$$

$$\ln(I_{IR}) = \ln(I_{0,IR}) - [\epsilon_{IR,Hb} C_{Hb} + \epsilon_{IR,HbO2} C_{HbO2}] d(t) \quad (9)$$

Applying a bandpass filter (in signal processing blocks 703 and 707) removes the non-time varying components, and allows Equations (8) and (9) to be rewritten as:

$$RD(t) = -[\epsilon_{RD,Hb} C_{Hb} + \epsilon_{RD,HbO2} C_{HbO2}] d(t) \quad (10)$$

$$IR(t) = -[\epsilon_{IR,Hb} C_{Hb} + \epsilon_{IR,HbO2} C_{HbO2}] d(t) \quad (11)$$

Figure 9 shows a plot of RD(t) versus IR(t). In Figure 9, an x axis 810 corresponds to IR(t) and a y axis 811 corresponds to RD(t). A straight line 812, having a positive slope, illustrates how the plot of RD(t) versus IR(t) would appear under ideal conditions of no noise, no scattering, and no motion artifacts. A curve 813 depicts a more realistic locus of points RD(t) versus IR(t) under normal measurement conditions. Figure 8 shows a plot of blood oxygen saturation versus the ratio of the RMS value of RD(t)/IR(t). Figure 8 shows an x axis 801 corresponding to blood oxygen saturation from 0% to 100% and a y axis corresponding to RMS(RD(t))/RMS(IR(t)) ranging from 0 to 3. A saturation curve 803 depicts the relationship between RMS(RD(t))/RMS(IR(t)) and blood oxygen saturation. The blood oxygen saturation is given by $\text{sat} = 100 * C_{HbO2} / (C_{Hb} + C_{HbO2})$. It is obtained by dividing Equation (10) by Equation (11) and solving for C_{HbO2} and C_{Hb} using the measured values of RD(t) and IR(t), and the known values of the absorption coefficients. Note that the unknown quantity d(t) is approximately the same for both red and infrared and thus divides out.

Detection and Removal of Motion Artifacts

Persons skilled in the art know that the data obtained during pulse oximetry measurements using red and infrared light are often contaminated due to motion. Identification and removal of these motion artifacts is often a prerequisite to any signal processing used to obtain blood oxygen saturation, pulse rate, or other physiological data. Figure 10 schematically illustrates an additive noise process

is shown as a series of peaks, comprising a first spectral peak 1104 at a fundamental frequency f_0 , a second spectral peak 1107 at a first harmonic f_1 and a third spectral peak 1110 at a frequency f_m . The spectrum of $IR(t)$, denoted mathematically as:

$$IR(\omega) = \mathcal{F}[IR(t)] \quad (13)$$

is shown as a series of peaks, comprising a first spectral peak 1103 at the fundamental frequency f_0 , a second spectral peak 1106 at the first harmonic f_1 and a third spectral peak 1109 at a frequency f_m . The ratio of the spectral components, given by $RD(\omega)/IR(\omega)$, is shown as a first ratio line 1105 at the fundamental frequency f_0 , a second ratio line 1108 at the first harmonic f_1 and a third ratio line 1111 at the frequency f_m . As discussed below, when there are no motion artifacts in the spectrum of Figure 11, all of the spectral peaks will occur at harmonic frequencies, and all of the ratio lines will have approximately the same height. Under conditions of no motion, difference in the height of the ratio lines will be due primarily to scattering effects. The spectral peaks 1110 and 1109 corresponding to the frequency f_m , which is not necessarily a harmonic of f_0 , represent peaks due to motion, and therefor having an amplitude different from that of the first spectral line 1105 and the second spectral line 1108.

One skilled in the art will recognize that the representations in Figure 11 have been idealized for the purposes of explanation. In particular, in actual measured data, especially data contaminated by noise and other undesired components, the frequencies of the spectral peaks of $RD(\omega)$ do not correspond exactly to the spectral peaks of $IR(\omega)$. Although corresponding frequencies will typically be quite close, variations of a few percent are not unexpected. Thus, for example, it will be obvious to one skilled in the art that, due to the imperfections in most measured data, the fundamental frequency f_0 found for $RD(\omega)$ will often be different from the fundamental frequency f_0 found for $IR(\omega)$. The same comments would apply to other harmonics (e.g., f_1 and f_2) as well. In one embodiment of the present invention, the frequencies f_0 , f_1 , f_2 (or equivalently ω_0 , ω_1 , ω_2), etc. (hereinafter the frequency peaks) correspond to the frequency peaks found in $RD(\omega)$, and the ratios $RD(\omega)/IR(\omega)$ are calculated using the values of $RD(\omega)$ and $IR(\omega)$ at those frequencies, regardless of whether they also

happen to correspond to a frequency peak in $IR(\omega)$. In another embodiment of the present invention, the frequency peaks correspond the frequency peaks found in $IR(\omega)$, and the ratios $RD(\omega)/IR(\omega)$ are calculated using the values of $RD(\omega)$ and $IR(\omega)$ at those frequencies, regardless of whether they also happen to correspond to a frequency peak in $RD(\omega)$. In yet another embodiment of the present invention, the frequency peaks of $RD(\omega)$ and $IR(\omega)$ are found separately, and the ratios $RD(\omega)/IR(\omega)$ are calculated by matching the frequency peaks of $RD(\omega)$ with the nearest frequency peaks of $IR(\omega)$.

In an ideal measurement, the red and infrared spectra are the same to within a constant scale factor. Thus, in an ideal measurement, all of the ratio lines 1105, 1108 and 1111 have substantially the same amplitude. Any differences in the amplitude of these lines is likely due to motion or other contaminations represented by $n(t)$ (including scattering effects). For each component, red and infrared, the model of Figure 9 can be expressed as:

$$\begin{aligned} S_1(t) &= A(t) + N(t) \\ S_2(t) &= rA(t)h(t) + \mu N(t)\eta(t) \\ &\approx rA(t) + \mu N(t) \end{aligned} \tag{14}$$

where $S_1(t)$ represents the infrared signal, $A(t)$ represents the desired infrared signal and $N(t)$ represents the noise signal. Likewise, $S_2(t)$ represents the measured red signal, r represents the ratio of red to infrared ($RD(\omega)/IR(\omega)$) expected in an uncontaminated measurement, and μ represents the ratio of red noise to infrared noise. The quantities $h(t)$ and $\eta(t)$ are primarily due to scattering, and thus required because, strictly speaking, $A(t)$ and $N(t)$ in the red channel and infrared channels are not simply related by a constant. However, for most purposes, the quantities $h(t)$ and $\eta(t)$ are sufficiently close to unity that they can be ignored.

Introducing an arbitrary scaling factor α into the equation for S_1 , and then subtracting the two equations yield (for notational convenience, the time dependence of S , A and N will not be explicitly shown):

$$\alpha S_1 - S_2 = A(\alpha - r) + N(\alpha - \mu) \tag{15}$$

Two special cases arise from Equation (17). First, when $\alpha=r$, Equation (17) reduces to:

$$N = \frac{\alpha S_1 - S_2}{r - \mu} \quad (16)$$

Second, when $\alpha=\mu$, Equation (17) reduces to:

$$A = \frac{\alpha S_1 - S_2}{\mu - r} \quad (17)$$

5 The values of μ and r can be found from the ratio of $RD(\omega)/IR(\omega)$ as shown in Figure 11 and the following two observations. First, since r is the coupling coefficient between red and infrared (the ratio of red to infrared) then r is expected to be reasonably constant over short periods of time. Likewise, μ is expected to be relatively constant because it is merely the coupling coefficient between the noise in the red and infrared signals. Second, the condition $\mu=r$ is not expected to occur because that would mean that the saturation due to arterial blood is equal in magnitude to the saturation due to venous blood. One skilled in the art will recognize, that, except for short periods of time, arterial blood saturation and venous blood saturation cannot be the same, because a living body consumes oxygen from the blood as the blood passes from the arteries to the veins. Arterial blood and venous blood saturation can be the same for short periods of time, and even reversed, especially where blood pooling has occurred and a quick desaturation is taking place. It is always expected that μ is larger than r . Therefore, in one embodiment of the present invention, the value of μ corresponds to the largest peak in Figure 11 and the value of r corresponds to the smallest peak of Figure 11. Further, the presence of motion artifacts in the data are easily detectable by examination of the relationship between μ and r .

20 In a preferred embodiment, the value of μ is found by classifying the ratio peaks according to a ratio threshold g . The ratio threshold g is computed identifying the first N ratio lines R_N associated with the first N spectral peaks. The ratio threshold g is then computed as a modified center of mass for the R_N lines according to the following equation.

$$g = \frac{N}{\sum_{i=0}^{N-1} \frac{1}{R_i}}$$

Each ratio line is then compared with the ratio threshold g . Only those ratio lines whose magnitude is larger than the ratio threshold g are included in a set Y of ratio lines. Only ratio lines in the set Y are used in the calculation of μ . In one embodiment, the value of μ is the magnitude of the largest ratio peak in the set of ratio peaks R_i for $i = 0 \dots N$. In an alternate embodiment, the value of μ is the magnitude of the ratio peak corresponding to the largest spectral peak in the set Y .

The values of μ and r are used to determine whether motion artifacts are present. In one embodiment, the ratio μ/r is calculated. If the ratio is close to unity, then, to within a constant scaling factor, the spectrum $RD(\omega)$ is approximately the same as the spectrum $IR(\omega)$ and thus there are no motion artifacts. If, on the other hand, the ratio μ/r is not close to unity, then the shape of the spectrum $RD(\omega)$ is different from the spectrum $IR(\omega)$, signaling the presence of motion artifacts, and thus the spectrum must be scrubbed according to Equation (17).

In a preferred embodiment, a delta is computed by subtracting the magnitude of the smallest ratio line from the magnitude of the largest ratio line. If the delta is smaller than a threshold value, then the spectrum $RD(\omega)$ is approximately the same as the spectrum $IR(\omega)$ and thus there are no motion artifacts, but only variations due to scattering. If, on the other hand, the delta $\mu - r$ is greater than the threshold value, then the shape of the spectrum $RD(\omega)$ is different from the spectrum $IR(\omega)$, signaling the presence of motion artifacts, and thus the spectrum must be scrubbed according to Equation (19).

Figure 12 shows a block diagram of a signal processing system that implements the motion detection and spectrum scrubbing operations in accordance with one aspect of the present invention. In Figure 12, an input from a single sensor 1202 that receives red and infrared light is fed into a demultiplexer 1204 which separates the red and infrared signals. The red signal is fed into a filter 1206 which removes unwanted

001140" 88524560

spectral components. The output of the filter 1206 is normalized (as is described in the text describing Figure 7) by the series combination of a log amplifier 1208, and a bandpass filter 1210. The output RD(t) of the bandpass filter 1210 is fed into a Fourier transform block 1214. The output of the transform block 1214 is fed into the numerator term of a divider 1230. The infrared output from the demultiplexer 1204 is processed, in the same fashion as the red signal, by the series combination of a filter 1220, a log amplifier 1222, a bandpass filter 1224, and a Fourier transform block 1228. The output of the Fourier transform block 1228 is fed into a denominator input of the divider 1230. An output of the divider 1230 is fed into a process block 1240 which determines μ , and r , and which computes α according to the flowchart of Figure 13. An output of the process block 1240 is fed as an input to a time domain waveform scrubber 1242. The time domain waveform scrubber 1242 has three input terminals, A, B, and D, and a single output terminal C. The time domain scrubber terminal A is connected to the output of the bandpass filter 1210. The time domain scrubber terminal B is connected to the output of the bandpass filter 1224. The time domain scrubber terminal D is connected to the α output of the process block 1240. Inside the time domain scrubber 1242, the terminal A is connected to a signal input of a gain controlled amplifier 1244. A gain control input of the amplifier 1244 is connected to the scrubber terminal D. The scrubber terminal B is connected to a plus input of an adder 1246. An output of the amplifier 1244 is connected to a minus input of the adder 1246. An output of the adder 1246 is connected to a Fourier transform block 1248. An output of the Fourier transform block 1248 is connected to the scrubber output terminal C.

One skilled in the art will recognize that the linearity of the Fourier transform allows the scrubbing operation to be carried out in the frequency domain as well. A frequency domain scrubber 1260 is also shown in Figure 12. The frequency domain scrubber 1260 has the same four terminals, A, B, C, and D, as the time domain scrubber 1242.

Inside the frequency domain scrubber 1260, the terminal A is connected to a signal input of a Fourier transform block 1262. The output of the Fourier transform block 1262 is connected to a signal input of a gain controlled amplifier 1266. A gain

control input of the amplifier 1266 is connected to the scrubber terminal D. The scrubber terminal B is connected to a Fourier transform block 1264. An output of the transform block 1264 is connected to a plus input of an adder 1268. An output of the amplifier 1266 is connected to a minus input of the adder 1268. An output of the adder 1268 is connected to the scrubber output terminal C.

Regardless of whether the time domain scrubber 1242 or the frequency domain scrubber 1260 is used, the scrubber output C is a plethysmographic waveform in the frequency domain at a terminal 1249. Ideally, the waveform at terminal 1249 is cleaner (e.g., has a better signal to noise ratio) than the waveform at either scrubber input A or scrubber input B. The waveform at terminal 1249 can be displayed on a display (not shown) or sent to a rule based pulserate detector 1250 and/or a transform based pulserate detector 1252.

Figure 13 is a flowchart which illustrates the process steps performed by the signal processing block 1240 in Figure 12. The flowchart of Figure 13 begins at a start block 1302 and proceeds to a process block 1304. In the process block 1304, the spectrum $F(\omega)=RD(\omega)/IR(\omega)$ is searched for the largest ratio line μ and smallest ratio line r and the frequencies f_μ and f_r at which those two lines occur. The process then advances to a process block 1306 where the difference, delta $d = \mu - r$ is computed. The process then proceeds to a decision block 1308. If, in the decision block 1308, the delta d is greater than a threshold value, then motion artifacts are present and the process advances to a decision block 1312 to continue the calculation of α . Otherwise, if in the process block 1308, the delta d is less than the threshold value, then no scrubbing is necessary and the process advances to a process block 1310. Since both μ and r are ratios, they are dimensionless. The delta d is also dimensionless. In a preferred embodiment, the threshold value is 0.5. In the process block 1310, the value of α is set to 0, which essentially disables the scrubber. In the decision block 1312, the frequencies f_μ and f_r are compared. If the two frequencies are close together, then the process advances to a process block 1314; otherwise, the process advances to a process block 1316. In the process block 1314 the value of α is set to $\alpha=(\mu+r)/2$. In the process block 1316 the value of α is set to $\alpha=\mu$. The process blocks 1310, 1314 and 1316 all advance to a process block 1318 where the

value of α is sent to the scrubber. Upon completion of the process block 1318, the process jumps back to the process block 1304 to recalculate α .

One skilled in the art will recognize that the flowchart in Figure 13 can be modified to perform additional functions. For example, upon detecting that motion artifacts are present (during the transition to the decision block 1312), an indicator can be lit, or an alarm can be sent, to warn the medical clinician that motion artifacts were present. In yet another embodiment, upon transitioning to the process block 1312, the delta d could be examined against a second threshold to determine whether the motion artifacts were so severe that further processing was impossible.

Rule Based Pulserate Detection

In addition to measuring blood oxygen saturation, a pulse oximeter is able to perform continuous monitoring of a patient's pulserate. As shown in Figure 6, each heartbeat forces blood into the arteries and that increase in blood is detected by the plethysmographic apparatus. Thus, the scrubbed spectrum present at the terminal 1250 in Figure 12 contains some of the information that would be found in the Fourier spectrum of an electrocardiograph (EKG).

Figure 14A shows an ideal spectrum $F(\omega)$ of a clean plethysmographic wave from a heart that is beating with a very regular beat. The figure shows an x axis corresponding to frequency and a y axis corresponding to the magnitude of the spectral components. A curve 1412 shows $|F(\omega)|$. It is well known, that the waveform of a human heartbeat is not a pure sine wave, and thus the curve 1412 is not a single spectral line, but rather a first spectral line at a fundamental frequency f_0 and a series of decreasing harmonics at $2f_0$, $3f_0$, etc. Clearly, under these conditions, the frequency f_0 corresponds to the pulserate.

Often the ideal waveform of Figure 14A is not seen because the heart is beating irregularly or because the cardio-vascular system of the subject is producing a large dicrotic notch. This leads to a spectrum in which the largest spectral line is not necessarily the pulserate. Figure 14B shows one example of such a waveform. Like Figure 14A, Figure 14B shows an x axis corresponding to frequency, and a y axis corresponding to amplitude. A curve 1422 shows $|F(\omega)|$. However, unlike the curve 1412, the curve 1422 shows a spectral line at a fundamental

frequency f_0 , and a series of harmonics f_1 and f_2 having amplitudes larger than the amplitude of the fundamental, with f_2 being the largest. The curve 1422 illustrates the folly of attempting to determining pulserate merely by finding the largest spectral line. Such an algorithm, applied to the curve 1422 would report a pulserate that was

5

The spectrum shown in curve 1422 is commonly seen in plethysmographic waveforms and corresponds to a frequency modulated (FM) heartbeat. In accordance with one aspect of the present invention, a rule based method for determining the pulserate of a heart producing the spectrum of Figure 14B is disclosed. The rule based method is based on a time domain model (a "stick model") plotted in Figure 14C. This elegantly simple model captures the essential feature of the plethysmographic waveform. Figure 14C shows an x axis 1401 corresponding to time, and a y axis 1402 corresponding to the amount of blood being forced into the arteries by a heart. Figure 14C further shows two overlapping waveforms. A first waveform 1403 shows to blood being forced into the arteries during a first time interval T_1 . A second waveform 1404 shows blood being forced into the arteries during a second time interval T_2 . The two time intervals, T_1 and T_2 , do not overlap and the total period of the sum of the two waveforms is $T_1 + T_2$. The sum of the two waveforms represents a heart that is beating at two different pulserates on alternate beats. For example, if the heartbeats were numbered, then on every even numbered beat, the heartbeat would last T_1 seconds. On every odd numbered beat, the heartbeat would last T_2 seconds. This is not an unusual occurrence, and there are physiological reasons why this occurs. The spectrum shown in Figure 14B is essentially the spectrum of the superposition of the waveforms 1403 and 1404.

10

15

20

25

Amplitude modulation (AM) of the plethysmographic waveform is also possible and common. Amplitude modulation occurs primarily when the heart beats with different strength on different heartbeats. Figure 15 shows a sample spectrum $F(\omega)$ that exhibits the effects of AM. Figure 15 shows a frequency axis 1501 and a spectrum axis 1502. The spectrum consists of a series of spectral peaks 1503 and sidebands 1504. One skilled in the art will recognize this as a typical AM spectrum of a carrier and its associated modulation sidebands. Under some conditions, of high

30

pulserate and substantial modulation bandwidth, the sidebands 1504 due to one spectral peak 1503 can overlap the sidebands due to an adjacent spectral peak. This overlap significantly complicates the waveform (not shown).

In accordance with one aspect of the present invention, the pulserate can be determined in the presence of FM and AM distortions by classifying the spectrum as one of five categories grouped into three cases. The five categories are illustrated as idealized graphs in: Figure 16A, illustrating Case I; Figure 16B, illustrating Case II; and Figure 16C, illustrating Case III.

Figure 16A shows a plot 1600 having an x axis 1601 corresponding to frequency and a y axis 1602 corresponding to the magnitude of the spectrum. Figure 16A also shows a first spectral line 1603, a second spectral line 1604 and a third spectral line 1605. The three spectral lines 1603, 1604, and 1605 show a monotonically decreasing amplitude where the decrease is approximately linear.

Figure 16B shows a first plot 1610 having an x axis 1611 corresponding to frequency and a y axis 1612 corresponding to the magnitude of the spectrum. The first plot 1610 also shows a first spectral line 1613, a second spectral line 1614 and a third spectral line 1615. The third spectral line 1615 has the smallest amplitude of the three lines. The second spectral line 1614 has the largest amplitude of the three lines, and its amplitude rises significantly above a line drawn from the first spectral line 1613 to the third spectral line 1615.

Figure 16B also shows a second plot 1620 having an x axis 1621 corresponding to frequency and a y axis 1622 corresponding to the magnitude of the spectrum. The second plot 1620 also shows a first spectral line 1623, a second spectral line 1624 and a third spectral line 1625. The first spectral line 1623 has the smallest amplitude of the three lines. The second spectral line 1624 has the largest amplitude of the three lines, and its amplitude rises significantly above a line drawn from the first spectral line 1623 to the third spectral line 1625.

Figure 16C shows a first plot 1630 having an x axis 1631 corresponding to frequency and a y axis 1632 corresponding to the magnitude of the spectrum. The first plot 1630 also shows a first spectral line 1633, a second spectral line 1634 and

a third spectral line 1635. The amplitudes of the three spectral lines are monotonically increasing, and the increase is approximately linear.

Figure 16C also shows a second plot 1640 having an x axis 1641 corresponding to frequency and a y axis 1642 corresponding to the magnitude of the spectrum. The second plot 1640 also shows a first spectral line 1643, a second spectral line 1644 and a third spectral line 1645. The third spectral line 1645 has the smallest amplitude of the three lines. The second spectral line 1644 has the largest amplitude of the three lines, and its amplitude is significantly below a line drawn from the first spectral line 1643 to the second spectral line 1645.

In accordance with one aspect of the present invention, the pulserate is determined by identifying the largest three spectral lines, then matching the spectrum to one of the idealized spectra shown by the plots 1600, 1610, 1620, 1630, or 1640, and then applying one of a set of rules to determine the pulserate. It will be understood by one skilled in the art that, although the frequencies of the spectral shown in the plots 1600, 1610, 1620, 1630, or 1640 appear to be harmonically related. In practice the spectral lines may not correspond to frequencies which are harmonics.

The details of the rule based process are shown in the flowchart of Figure 18. Figure 18 begins at a start block 1802 and proceeds to an initialization process block 1804. In the block 1804, the values of the pulserate, p , and confidence factor, s , are set to zero. When the process reaches an exit block, p will contain the pulserate (or zero if no pulserate was found), and σ will contain a confidence factor indicating related to the pulserate (or zero if no pulserate was found). After completing the initialization block 1804, the process advances to a search process block 1805 where the spectrum $|F(\omega)|$ is searched for the first three spectral peaks. After finding the peaks, the process advances to a decision block 1806 where the process checks the number of spectral peaks actually found. If, in the decision block 1806, the number of peaks is less than three, then the process advances to a decision block 1808; otherwise, the process jumps forward to a process block 1812. If, in the process block 1808, the number of peaks is greater than zero, then the process advances to a process block 1810; otherwise, the process jumps to an exit block. In the process block 1810, the value of p is set to the frequency corresponding to the largest of the spectral

peaks, the confidence value is set to 10, and the process then advances to the exit block.

5 In the process block 1812, the first three spectral peaks are sorted by magnitude, and the values assigned to variables A_0 , A_1 , and A_2 such that A_0 is the magnitude of the largest peak, A_1 is the magnitude of the middle peak, and A_2 is the magnitude of the smallest peak. Also, in the process block 1812, variables f_0 , f_1 , and f_2 , representing the frequencies corresponding to A_0 , A_1 and A_2 respectively, are set. Upon completion of the process block 1812, the process advances to a decision block 1814. In the decision block 1814, if A_0 is greater than or equal to $1.2*(A_1+A_2)$ and f_0 is less than 250, then the process advances to a process block 1816; otherwise the process jumps to a decision block 1824. In the process block 1816, the value of p is set to $p = f_0$, and the process then advances to a decision block 1818. In the decision block 1818, the values of f_0 , f_1 , and f_2 are checked to see if they are harmonics of one another. In a preferred embodiment, this is done by checking to see whether a frequency f_i is within ten beats per minute of being a integer multiple of another frequency f_j (where $i, j = 0, 1, \text{ or } 2$). If the decision block 1818 detects that the frequencies are harmonics, then the process advances to a process block 1820; otherwise, the process advances to a process block 1822. In the process block 1820, the value of σ is set to 60, and the process then advances to the decision block 1824. In the process block 1822, the value of σ is set to 50 and the process then advances to the decision block 1824.

20 In the decision block 1824, if $A_0 < 1.2*(A_1+A_2)$, then the process advances to a decision block 1826, otherwise the process advances to the exit block. In the decision block 1826, if $(f_0 < f_1)$ and $(f_0 < f_2)$, then the process advances to a decision block 1828; otherwise the process advances to a decision block 1938. In the decision block 1828, if the frequencies f_0 , f_1 , and f_2 are harmonics, then the process advances to a decision block; otherwise, the process advances to a process block 1836. In the process block 1836, the value of p is set to $p=f_0$, the value of σ is set to 90, and the process then advances to the decision block 1838. In the decision block 1830, if f_0 is less than 45 beats per minute, then the process advances to a process block 1834; otherwise, the process advances to a process block 1832. In the process block 1832,

the value of p is set to $p=f_0$, the value of σ is set to $\sigma=80$, and the process then advances to the decision block 1838. In the process block 1834, the value of p is set to $p = (f_0+f_1+f_2)/3$, the value of σ is set to $\sigma=70$, and the process then advances to the decision block 1838.

5 In the decision block 1838, if $f_0 > f_1$ or $f_0 > f_2$, then the process advances to a decision block 1840; otherwise, the process advances to a decision block 1846. In the decision block 1840, if $(f_0 > f_1)$ and $(f_0, f_1 \text{ and } f_2 \text{ are harmonics})$ and $(A_0 < 1.7A_1)$ and $(30 < f_1 < 130)$ then the process advances to a decision block 1842; otherwise, the process advances to a process block 1844. In the process block 1842, the value of
10 p is set to $p = f_1$, the value of σ is set to $\sigma=100$, and the process then advances to the decision block 1848. In the process block 1844, the value of p is set to $p = f_0$, the value of σ is set to $\sigma=110$, and the process then advances to the decision block 1848.

In the decision block 1848, if $(f_0, f_1 \text{ and } f_2 \text{ are harmonics})$ and $f_0 < 100$ and $(A_1+A_2)/A_0 > 1.5$), then the process advances to a process block 1852; otherwise, the
15 process advances to a process block 1850. In the process block 1852, the value of p is set to $p = (f_0 + f_1 + f_2)/3$, the value of σ is set to $\sigma=120$, and the process then advances to the exit block. In the process block 1850, the value of p is set to $p = f_0$, the value of σ is set to $\sigma=130$, and the process then advances to the exit block.

As stated previously, when the process shown in Figure 18 reaches the exit
20 block, p contains the pulserate, and σ contains the confidence factor. The confidence factor is a number indicating the likelihood that the value of p accurately represents the actual pulserate of the patient.

Transform Based Pulserate Detection

In accordance with another aspect of this invention, the pulserate can be
25 determined in the presence of FM and AM distortions by using a pleth to pulserate transform (PPRT). Figure 17 shows a schematic of a signal processing system that implements a PPRT. In Figure 17, a time domain plethysmographic waveform $f(t)$ is fed into an input 1701. The signal at the input 1701 is fed into a Fourier transform block 1702 which forward transforms $f(t)$ into the frequency domain. An output of
30 the block 1702 is expressed mathematically as $F(\omega)=\mathcal{F}[f(t)]$. The output of the block 1702 is fed into a magnitude block 1703 which finds the magnitude of the signal

09547588-04100
001140-88524560

$F(\omega)$. An output of the magnitude block 1703, shown as a plot 1713, is fed into a second forward Fourier transform block 1704 which transforms the signal $|F(\omega)|$ into a signal $G(x)$ where $G(x) = \mathcal{F}[|F(\omega)|]$ and $G(x)$ is a complex number. The output of the block 1704 is fed into a block 1705 which extracts the real portion of $G(x)$. The real portion of $G(x)$ is then fed into a $1/x$ mapping block 1706. An output of the mapping block 1706 is fed into a pulserate detector block 1707. A pulserate output from the detector block 1706 is sent to a display 1708.

In an alternate embodiment, the magnitude block could be replaced by a block which extracts the real portion of the waveform. Likewise, the block 1705 which extracts the real portion of $G(x)$ could be replaced by a magnitude block which extracts $|G(x)|$.

One skilled in the art will recognize that the output of the magnitude block 1703 is merely the absolute value of the Fourier transform of the plethysmographic wave $f(t)$ on a point by point basis. The graph 1713 shows this signal as a series of spectral lines of varying amplitudes. In many cases, this spectrum will be similar to that shown in Figure 14B, and has a fundamental frequency f_0 , and a series of harmonics f_1 and f_2 of various amplitudes. As shown in Figure 14B, any attempt at determining pulserate merely by finding the largest spectral line will lead to erroneous results. Further, the clean waveform of Figure 14B, showing a series of spectral peaks, will often be contaminated by AM sidebands as shown in Figure 15. Thus the fundamental periodic nature of the heartbeat is not always readily apparent in the spectrum of plot 1713. This is the reason for the second Fourier transform in process block 1704.

The nature of the Fourier transform is to identify and quantify the periodic nature of a function. If the waveform shown in the plot 1713 were in the time domain, rather than the frequency domain, then the series of pulses (the spectral lines of the plot 1713) would correspond to a periodic train of pulses, having a fundamental frequency given by the pulse repetition frequency and modulated by the spectrum of the individual pulses. Mathematically, it does not matter that the waveform of the plot 1713 is not in the time domain. The Fourier transform can still be applied, and it will

still produce a very strong spectral line corresponding to the inherent periodicity, and corresponding component strength, of the waveform.

Thus, the operation of the block 1704, in performing a forward Fourier transform on a frequency domain waveform is mathematically viable, and yields the desired data. The only unique ramification of the fact that the transformed data is already in the frequency domain rather than the time domain is the effect on the x axis. It is well known to those skilled in the art, that the forward Fourier transform maps the x axis into $1/x$. This is most easily explained by noting that, normally, one would transform $f(t)$ into $F(\omega)$. Since $t = 1/\omega$ (to within a constant factor of 2π) it is clear that a $1/x$ mapping has occurred. In the present context, the $1/x$ mapping is undesirable because the data was already in the frequency domain. Thus the mapping must be undone by the process block 1706.

Once the waveform has been remapped in the process block 1707, it is a simple matter to find the desired pulserate in the process block 1707, because the pulserate will correspond to the largest spectral peak. Again, this occurs because the second Fourier transform "identifies" the dominant periodicity (e.g., the dominant string of harmonics) and collapses that periodicity into a single spectral line. The pulserate detector 1707 merely searches for the largest spectral peak and sends, to the display 1708, the frequency that corresponds to the largest peak.

In yet another embodiment, the process block 1707 looks for the existence of a spectral peak below 120 beats per minute. If a spectral peak below 120 beats per minute is found, then the frequency corresponding that peak is the pulserate. Of, on the other hand, no spectral peak below 120 beats per minute is found, then the process block 1707 finds the largest spectral peak in the original fourier spectrum that exists at the output of the Fourier transform block 1702. The pulserate is then the frequency corresponding to the largest spectral peak at the output of the Fourier transform block 1702.

In yet another embodiment, the ratio of the largest two peaks in the PPRT waveform 1716 can be used to generate a confidence factor that provides some indication of the accuracy of the computed pulserate. In a preferred embodiment, a contrast ratio is computed by dividing the magnitude of the largest peak in the PPRT

001140-8854550

waveform 1716 by the magnitude of the second largest peak in the PPRT waveform 1716. A large contrast ratio corresponds to high confidence that the computed pulserate is accurate. A contrast ratio near unity corresponds to low confidence that the computed pulserate is accurate.

5 Neural Network Embodiments

10 In yet another embodiment, much of the signal processing can be accomplished by a neural network. One skilled in the art will recognize that the signal processing associated with the removal of motion artifacts involves non-linear and linear processes. The frequency domain waveform scrubber 1260 and the time domain waveform scrubber 1242 are both linear processes. However, the calculation of α in Figure 12 is a non-linear process, in part because it includes the ratio operation represented by the process block 1230. The calculation of pulserate, either by the rule based method, or the PPRT method both involve ratios and are thus non-linear processes as well.

15 One skilled in the art will appreciate that other non-linear filtering processes can be used. In particular, any of these non-linear processes can be performed by a neural network as shown in Figure 19. Figure 19 depicts a general hardware block diagram of a pulse oximeter 299 that employs neural network processing. A sensor 300 has two light emitters 301 and 302, such as LED's. One LED 301 emitting light of red wavelengths and another LED 302 emitting light of infrared wavelengths are placed adjacent a finger 310. A photodetector 320, which produces an electrical signal corresponding to the attenuated visible and infrared light energy signals is, located near the LED's 301 and 302. The photodetector 320 is connected to front end analog signal conditioning circuitry 330.

20
25 The front end analog signal conditioning circuit 330 has outputs coupled to an analog to digital conversion circuit 332. The analog to digital conversion circuit 332 has outputs coupled to a digital signal processing and neural network signal extraction system 1934. The signal processing system 1934 provides the desired parameters as outputs for a display 336. Outputs for display are, for example, blood oxygen saturation, heart rate, and a clean plethysmographic waveform.

30

001140 884580

The signal processing system also provides an emitter current control output 337 to a digital-to-analog converter circuit 338 which provides control information for a set of light emitter drivers 340. The light emitter drivers 340 couple to the light emitters 301, 302. The signal processing system 1934 also provides a gain control output 343 for the front end analog signal conditioning circuitry 330.

Additional Embodiments

While one embodiment of a physiological monitor incorporating a processor of the present invention for determining a reference signal for use in a waveform scrubber, to remove or derive primary and secondary components from a physiological measurement has been described in the form of a pulse oximeter, it will be obvious to one skilled in the art that other types of physiological monitors may also employ the above described techniques.

In particular, one skilled in the art will recognize that in all cases, the Fourier transform disclosed above can be replaced by a Fast Fourier Transform (FFT), a Chirp-Z Transform, a wavelet transform, a discrete Fourier transform, or any other operation that produces the same or similar result.

Furthermore, the signal processing techniques described in the present invention may be used to compute the arterial and venous blood oxygen saturations of a physiological system on a continuous or nearly continuous time basis. These calculations may be performed, regardless of whether or not the physiological system undergoes voluntary motion.

Furthermore, it will be understood that transformations of measured signals other than logarithmic conversion and that the determination of a proportionality factor which allows removal or derivation of the primary or secondary signal portions for determination of a reference signal are possible. Additionally, although the proportionality factor r has been described herein as a ratio of a portion of a first signal to a portion of a second signal, a similar proportionality constant determined as a ratio of a portion of a second signal to a portion of a first signal could equally well be utilized in the processor of the present invention. In the latter case, a secondary reference signal would generally resemble $n'(t) = n_b(t) - rn_a(t)$.

One skilled in the art will realize that many different types of physiological monitors may employ the teachings of the present invention. Other types of physiological monitors include, but are in not limited to, electro-cardiographs, blood pressure monitors, blood constituent monitors (other than oxygen saturation) monitors, capnographs, heart rate monitors, respiration monitors, or depth of anesthesia monitors. Additionally, monitors which measure the pressure and quantity of a substance within the body such as a breathalyzer, a drug monitor, a cholesterol monitor, a glucose monitor, a carbon dioxide monitor, a glucose monitor, or a carbon monoxide monitor may also employ the above described techniques.

Furthermore, one skilled in the art will recognize that many of the signal processing techniques, and many of the filters disclosed herein are classification techniques. Many of the classification mechanisms herein involve classification of spectral lines and ratios of various spectral lines. Other classification schemes are possible within the spirit and scope of the invention.

Furthermore, one skilled in the art will realize that the above described techniques of primary or secondary signal removal or derivation from a composite signal including both primary and secondary components can also be performed on electrocardiography (ECG) signals which are derived from positions on the body which are close and highly correlated to each other.

Furthermore, one skilled in the art will realize that the above described techniques can also be performed on signals made up of reflected energy, rather than transmitted energy. One skilled in the art will also realize that a primary or secondary portion of a measured signal of any type of energy, including but not limited to sound energy, X-ray energy, gamma ray energy, or light energy can be estimated by the techniques described above. Thus, one skilled in the art will realize that the techniques of the present invention can be applied in such monitors as those using ultrasound where a signal is transmitted through a portion of the body and reflected back from within the body back through this portion of the body. Additionally, monitors such as echo-cardiographs may also utilize the techniques of the present invention since they too rely on transmission and reflection.

WHAT IS CLAIMED IS:

1. In a signal processor for processing at least two measured signals M_1 and M_2 each containing a primary signal portion S and a secondary signal portion N , said signals M_1 and M_2 having the following relationship:

5
$$M_1 = S_1 + N_1$$
$$M_2 = S_2 + N_2$$

where S_1 and S_2 , and N_1 and N_2 are related by:

$$S_1 \approx r_a S_2$$
$$N_1 \approx r_v N_2$$

10 and where r_a and r_v are coefficients, a method comprising the steps of:

determining a value for a coefficient c , such that an error value e , given by the relation $e = S_1 - (cM_1 - M_2)$ is partially minimized; and

using said coefficient c in a waveform scrubber to remove some of the signal N_1 from the measured signal M_1 and thereby producing an approximation A_1 to said signal S_1 , where $A_1 = cM_1 - M_2$.

15

2. The method of Claim 1, where A_1 , M_1 and M_2 are frequency domain signals.

3. The method of Claim 1, further comprising the step of displaying the resulting clean signal on a display.

20 4. The method of Claim 1, wherein said first and second signals are physiological signals, further comprising the step of processing said clean signal to determine a physiological parameter from said first and second measured signals.

5. The method of Claim 4, wherein said physiological parameter is arterial oxygen saturation.

25 6. The method of Claim 4, wherein said physiological parameter is an ECG signal.

7. The method of Claim 2, wherein the first portion of said measured signals is indicative of a heart plethysmograph, further comprising the step of calculating the pulse rate.

30

8. A physiological monitor comprising:

a first input configured to receive a first measured signal M_1 having a primary portion, S_1 , and a secondary portion N_1 ;

a second input configured to received a second measured signal M_2 having a primary portion S_2 and a secondary portion N_2 , said first and said second measured signals M_1 and M_2 being in accordance with the following relationship:

$$M_1 = S_1 + N_1$$

$$M_2 = S_2 + N_2$$

where S_1 and S_2 , and N_1 and N_2 are related by:

$$S_1 \approx r_a S_2$$

$$N_1 \approx r_v N_2$$

and where r_a and r_v are coefficients;

a first signal processor, said first signal processor configured to compute said r_a and said r_v using a transformed representation of said signal M_1 and a transformed representation of said signal M_2 ;

a waveform scrubber having a first input configured to receive said first measured signal, and having a second input to receive said second measured signal, said waveform scrubber providing an output corresponding to an approximation of S_1 ;

9. The physiological monitor of Claim 8, further comprising a second signal processor, said second signal processor configured to compute selected blood constituents from said first and second measured signals.

10. The physiological monitor of Claim 9, wherein said selected blood constituent is arterial blood oxygen saturation.

11. The physiological monitor of Claim 9, wherein said selected blood constituent is venous blood oxygen saturation.

12. The physiological monitor of Claim 9, wherein said selected blood constituent is carbon monoxide.

13. The physiological monitor of Claim 8, wherein said plurality of possible values correspond to a physiological concentration.

14. The physiological monitor of Claim 8, wherein said first signal processor comprises a neural network.

15. A physiological monitor attached to a living being having a heart beating at an unknown pulserate, said monitor comprising:

5 a detector responsive to physiological properties relating to heartbeats, said detector producing a detector output waveform;

a signal processor operatively coupled to said detector, said signal processor receiving said detector output waveform, said signal processor configured to:

10 transform said detector output waveform into a spectral domain waveform;

identify a series of spectral peaks and peak frequencies corresponding to said spectral peaks in said spectral domain waveform; and

15 apply a plurality of rules to said spectral peaks and said peak frequencies in order to determine an estimate for said pulserate.

16. The physiological monitor of Claim 15, wherein said signal processor comprises a neural network.

20 17. In a physiological monitor attached to a living organism, said organism having a heart beating at an unknown pulserate, said monitor having a detector responsive to physiological properties relating to heartbeats, said detector producing a detector output waveform, a method comprising the steps of:

25 transforming said detector output waveform into a spectral domain waveform;

identifying a series of spectral peaks and peak frequencies corresponding to said spectral peaks in said spectral domain waveform; and

30 applying a plurality of rules to said spectral peaks and said peak frequencies in order to determine an estimate for said pulserate.

18. A physiological monitor attached to a living organism, said organism comprising a heart beating at an unknown pulserate, said monitor comprising:

a detector responsive to physiological properties relating to said heartbeats, said detector producing a detector output waveform;

a signal processor operatively coupled to said detector, said signal processor receiving said detector output waveform, said signal processor configured to:

perform a first transform to transform said detector output waveform into a waveform in a first transform domain;

perform a second transform, to transform said waveform in said first transform domain into a waveform in a second transform domain;

search said waveform in said second transform domain for a largest spectral peak and a first frequency corresponding to said largest spectral peak; and

compute an estimate of said unknown pulserate from said first frequency.

19. The physiological monitor of Claim 18, wherein said first transform comprises a forward Fourier transform.

20. The physiological monitor of Claim 18, wherein said second transform comprises a Fourier transform into a spectral domain.

21. The physiological monitor of Claim 20, wherein said second transform further comprises a $1/x$ mapping of the coordinates in said spectral domain.

22. The physiological monitor of Claim 18, wherein said first transform is a Chirp-Z transform into a spectral domain.

23. The physiological monitor of Claim 18, wherein said second transform is a Chirp-Z transform into a spectral domain.

24. The physiological monitor of Claim 23, wherein said second transform further comprises a $1/x$ mapping of the coordinates in said spectral domain.

25. The physiological monitor of Claim 18, wherein said first transform is a transform into a spectral domain.

26. The physiological monitor of Claim 25, wherein said second transform is a transform into a spectral domain.

27. The physiological monitor of Claim 26, wherein said second transform further comprises a $1/x$ mapping of the coordinates in said spectral domain.

28. The physiological monitor of Claim 27, wherein said first transform further comprises performing an absolute value operation on said waveform in said first transform domain.

29. The physiological monitor of Claim 28, wherein said signal processor is further configured to:

search said waveform in said first transform domain for a highest spectral peak and a second frequency corresponding to said highest spectral peak; and

compute said estimate of said unknown pulserate from said second frequency if said first frequency is above a threshold frequency

30. In a physiological monitor attached to a living organism, said organism comprising a heart beating at an unknown pulserate, said monitor having a detector responsive to physiological properties relating to said heartbeats, said detector producing a detector output waveform, a method comprising the steps of:

performing a first transform to transform said detector output waveform into a waveform in a first transform domain;

performing a second transform, to transform said waveform in said first transform domain into a waveform in a second transform domain;

searching said waveform in said second transform domain for a largest spectral peak and a first frequency corresponding to said largest spectral peak; and

computing an estimate of said unknown pulserate from said first frequency.

IMPROVED SIGNAL PROCESSING APPARATUS AND METHOD

Abstract of the Invention

A method and an apparatus to analyze two measured signals that are modeled as containing desired and undesired portions such as noise, FM and AM modulation. Coefficients relate the two signals according to a model defined in accordance with the present invention. In one embodiment, a transformation is used to evaluate a ratio of the two measured signals in order to find appropriate coefficients. The measured signals are then fed into a signal scrubber which uses the coefficients to remove the unwanted portions. The signal scrubbing is performed in either the time domain or in the frequency domain. The method and apparatus are particularly advantageous to blood oximetry and pulserate measurements. In another embodiment, an estimate of the pulserate is obtained by applying a set of rules to a spectral transform of the scrubbed signal. In another embodiment, an estimate of the pulserate is obtained by transforming the scrubbed signal from a first spectral domain into a second spectral domain. The pulserate is found by identifying the largest spectral peak in the second spectral domain.

LWH-1256.R05:icb
041497

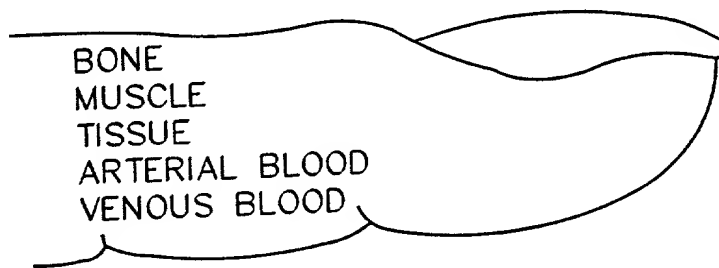


FIG. 1

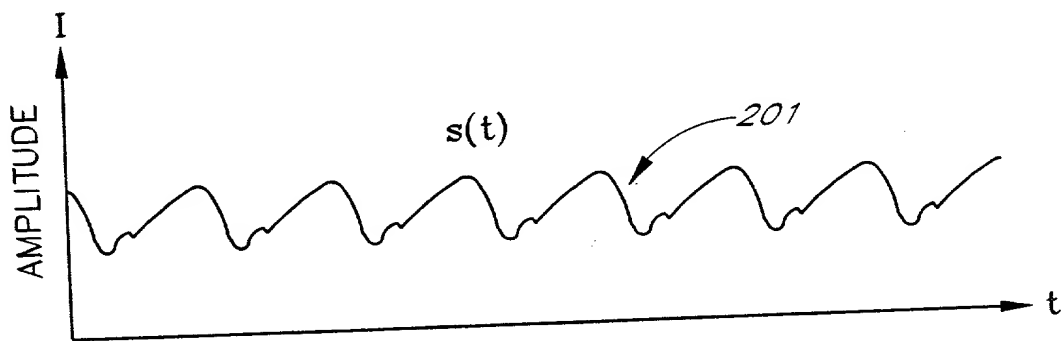


FIG. 2A

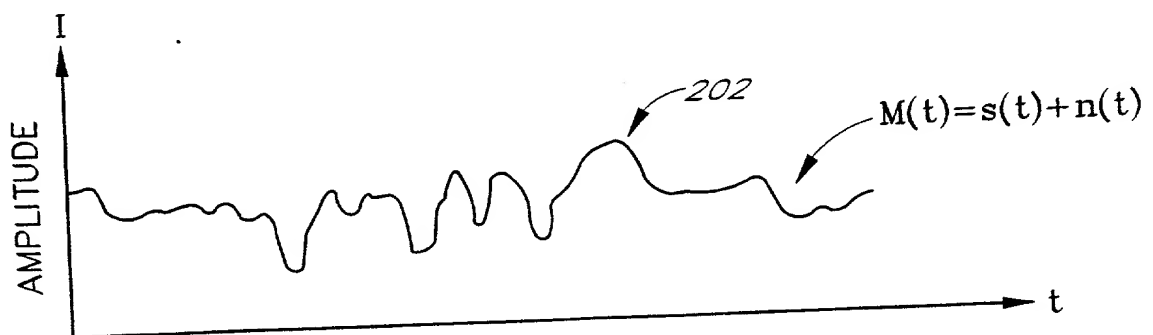


FIG. 2B

299

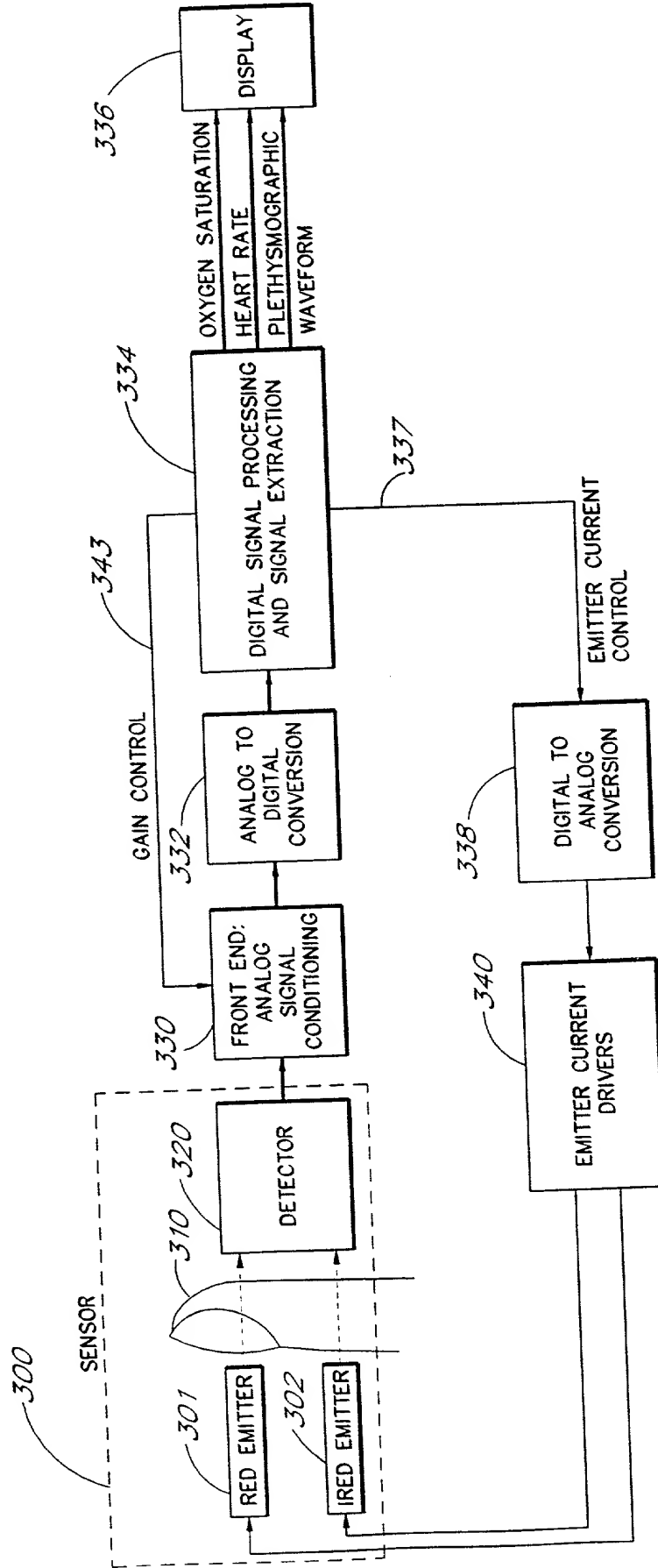


FIG. 3

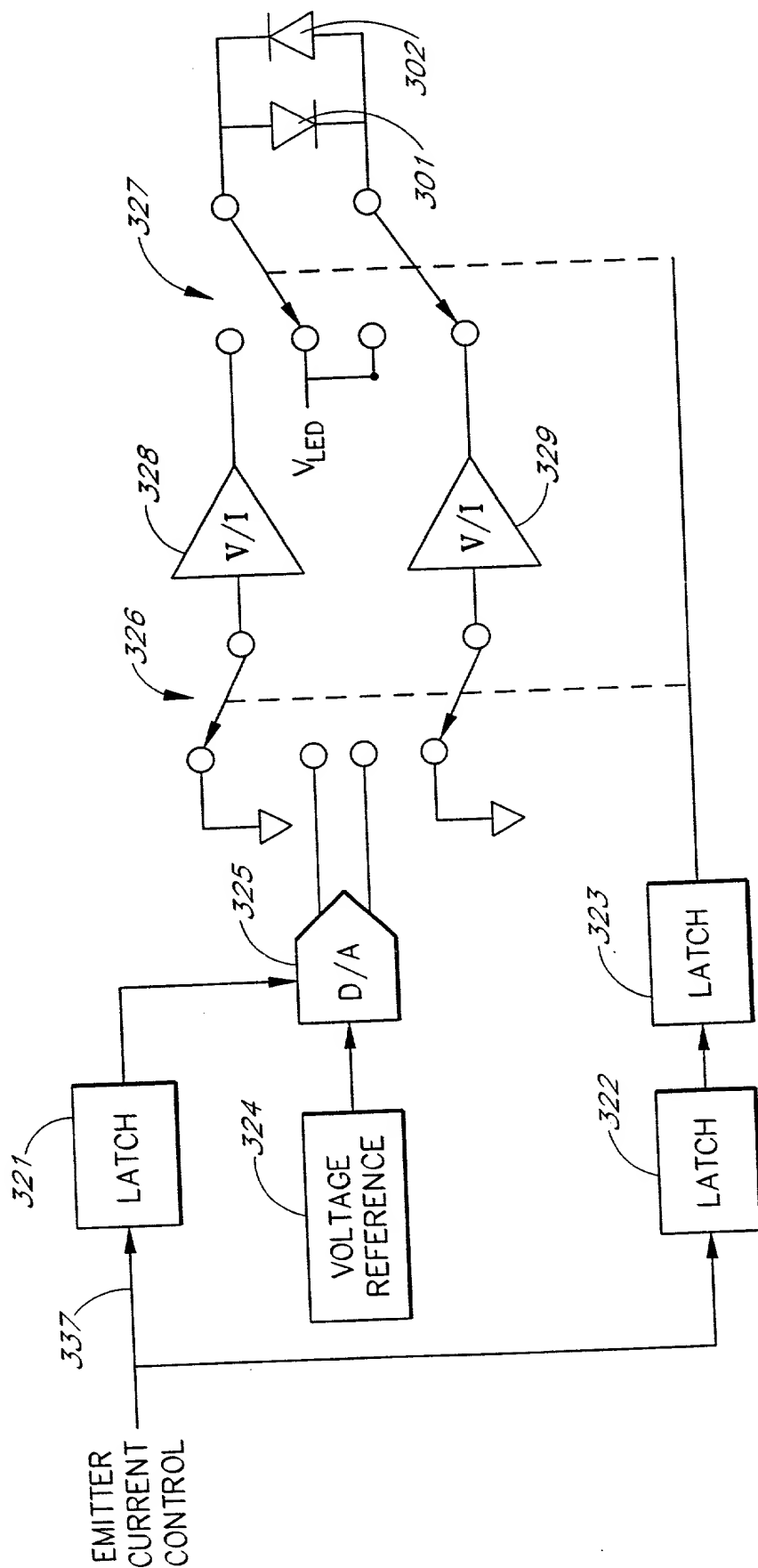


FIG. 4

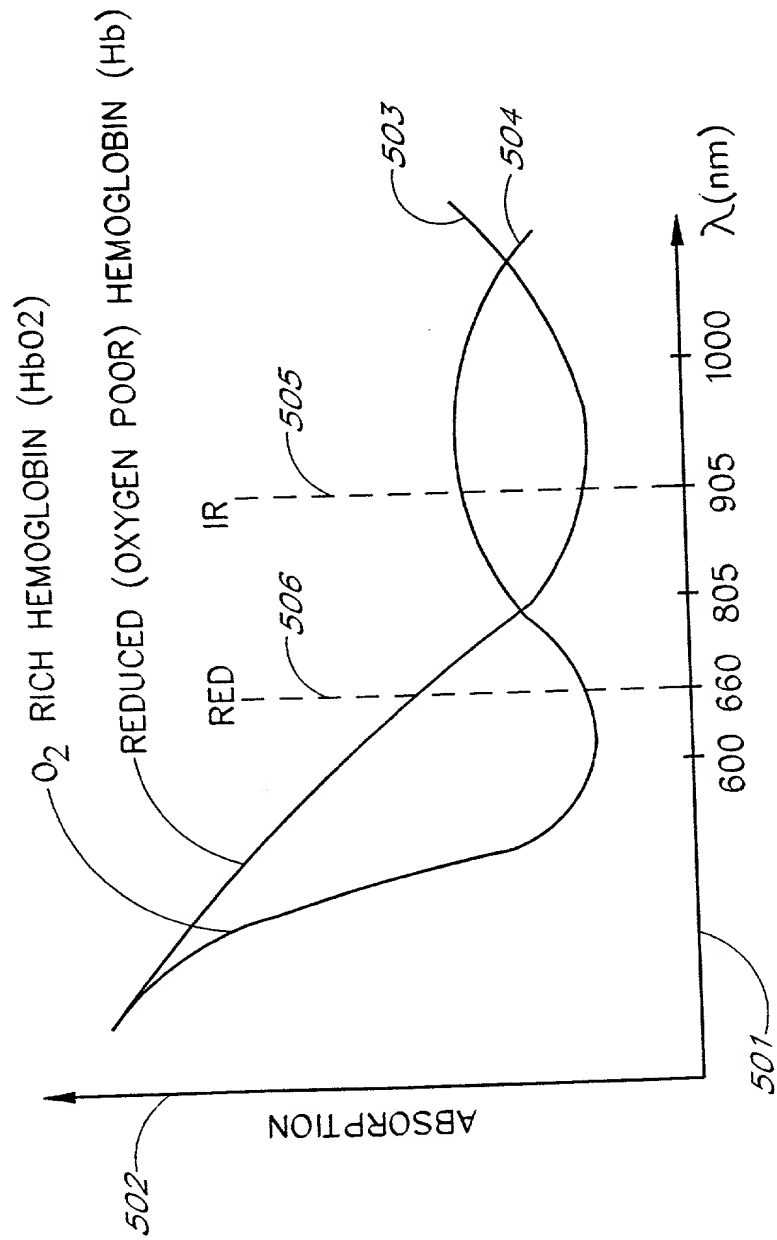


FIG. 5

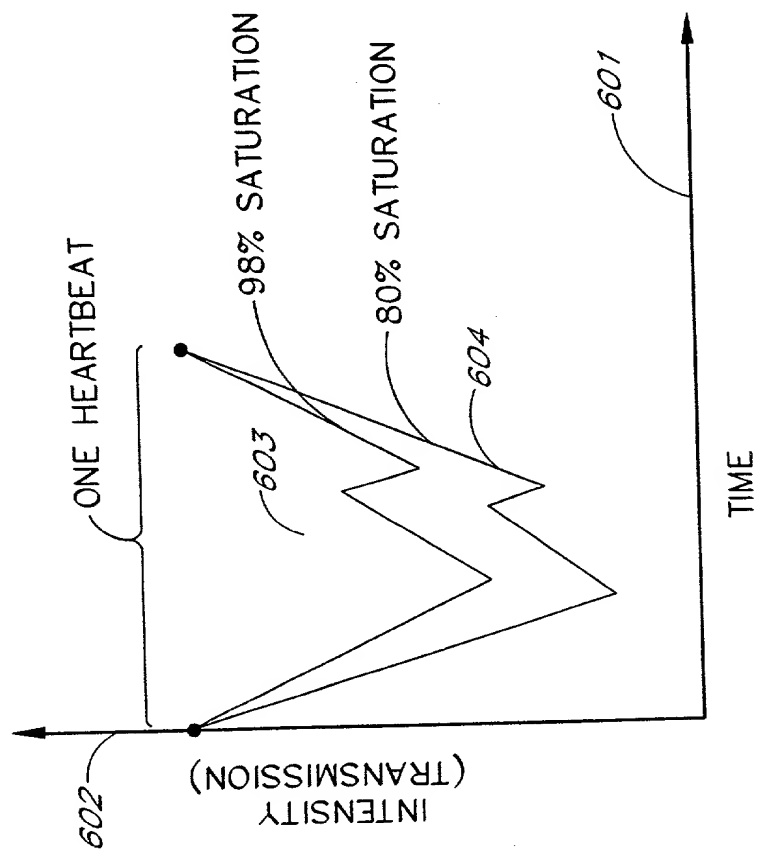


FIG. 6

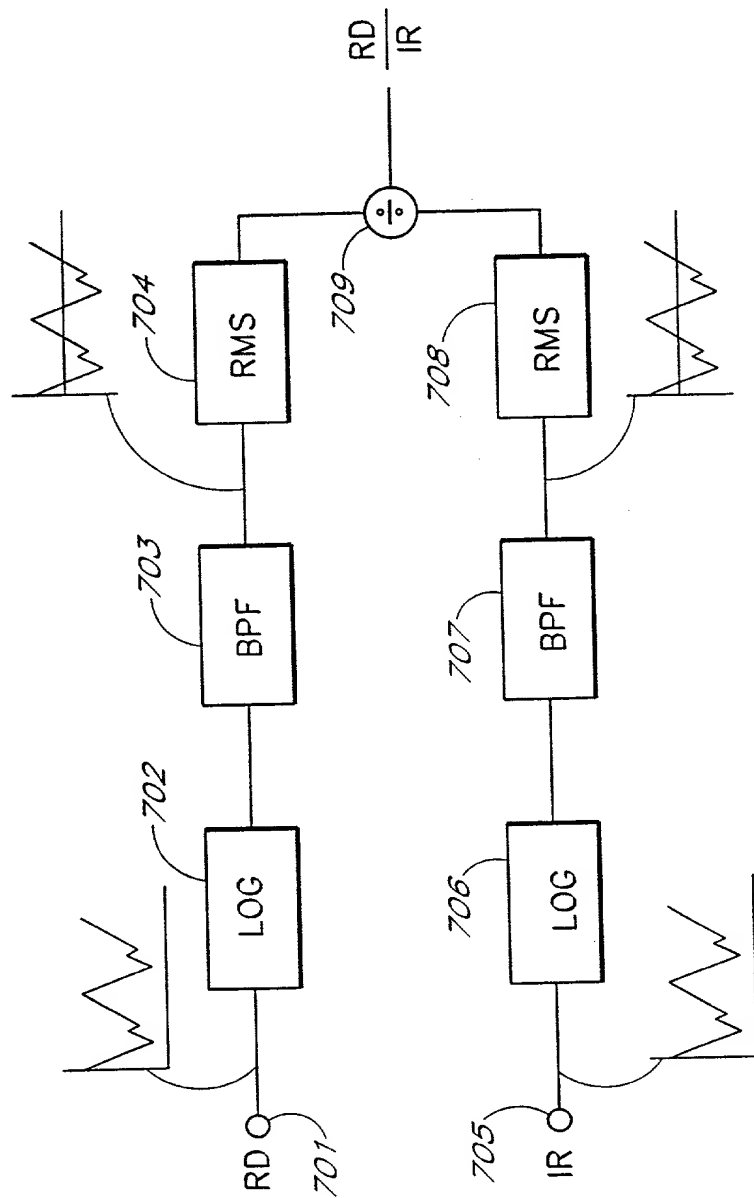


FIG. 7

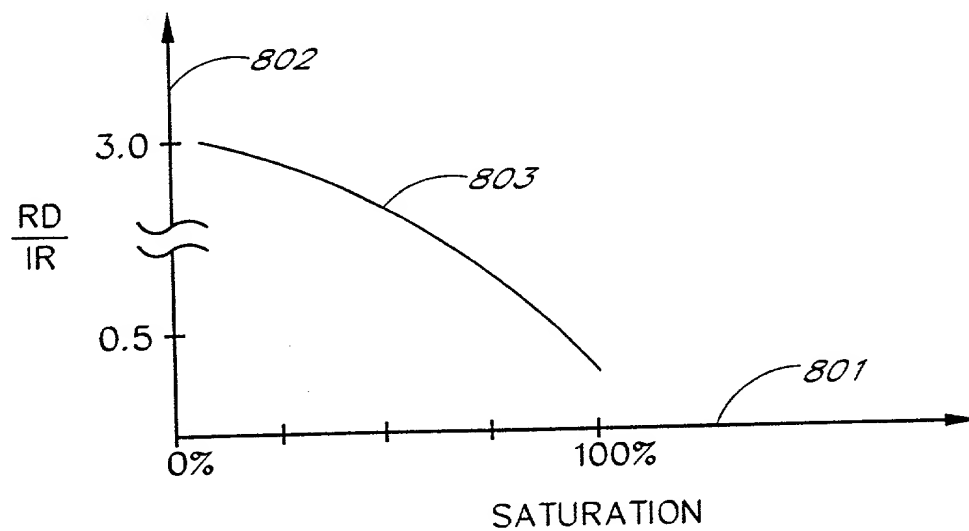


FIG. 8

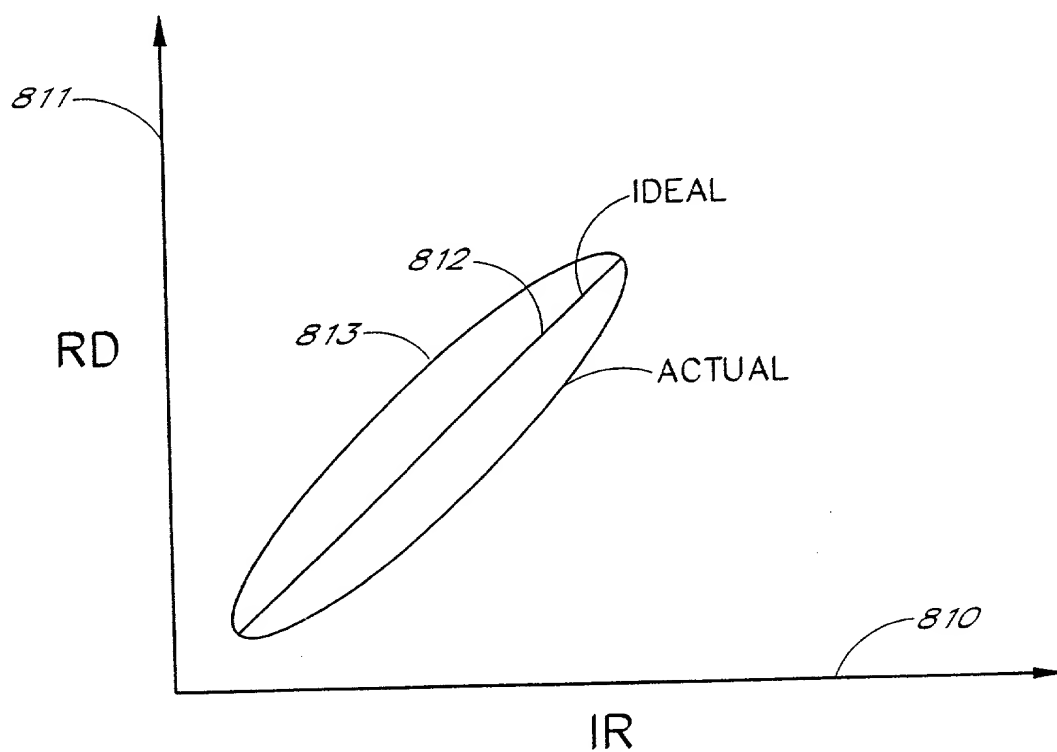


FIG. 9

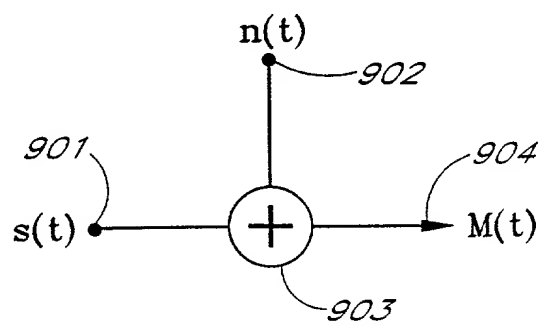


FIG. 10

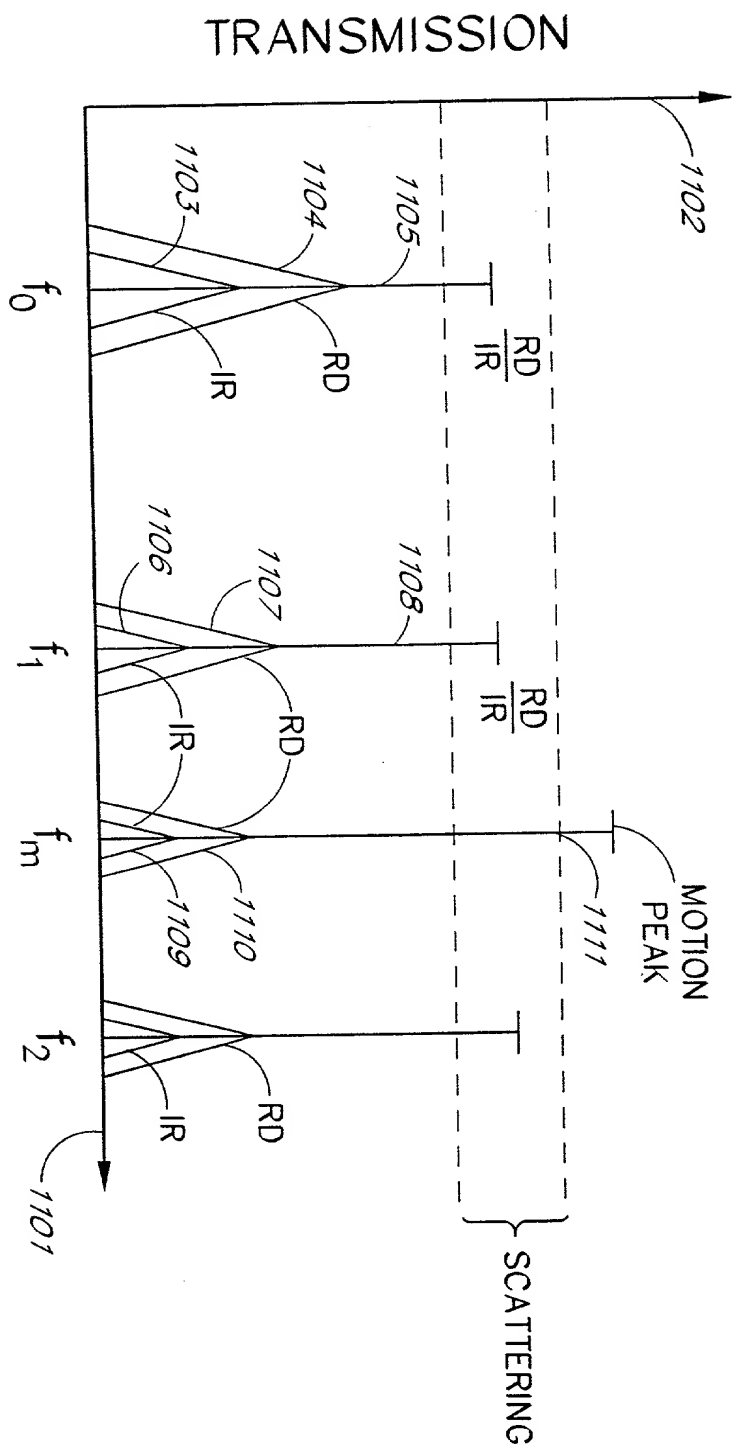


FIG. 11

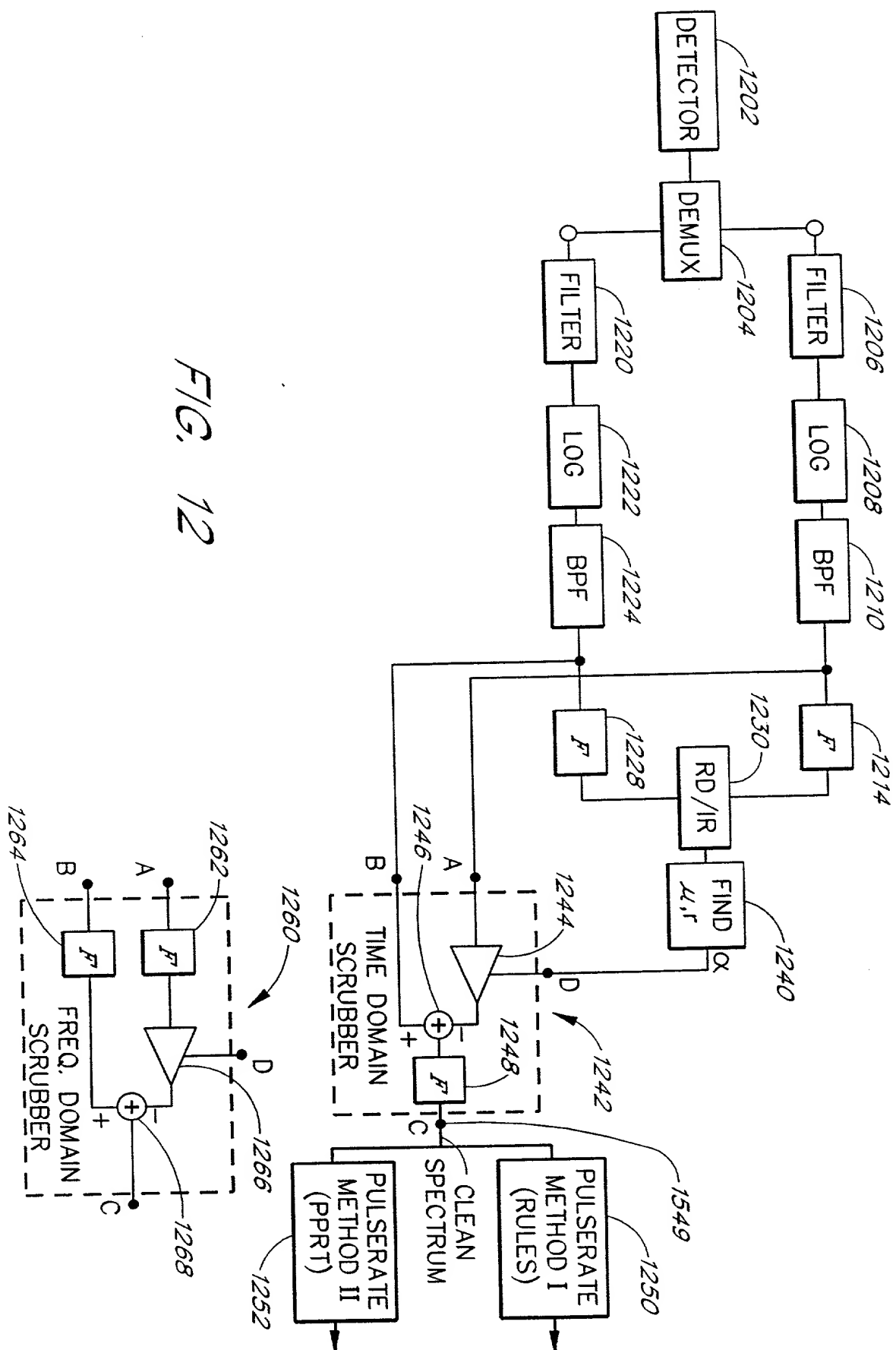


FIG. 12

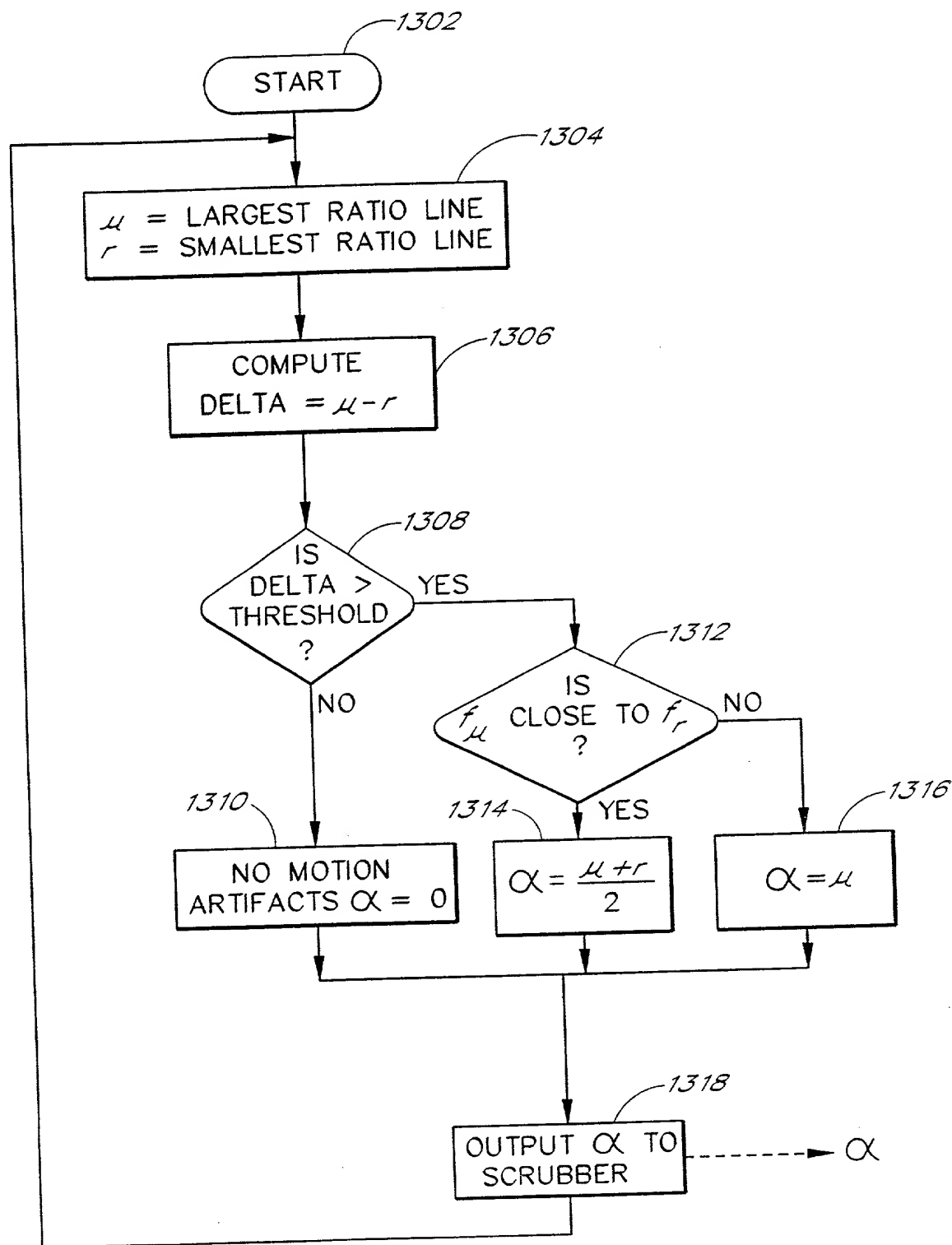


FIG. 13

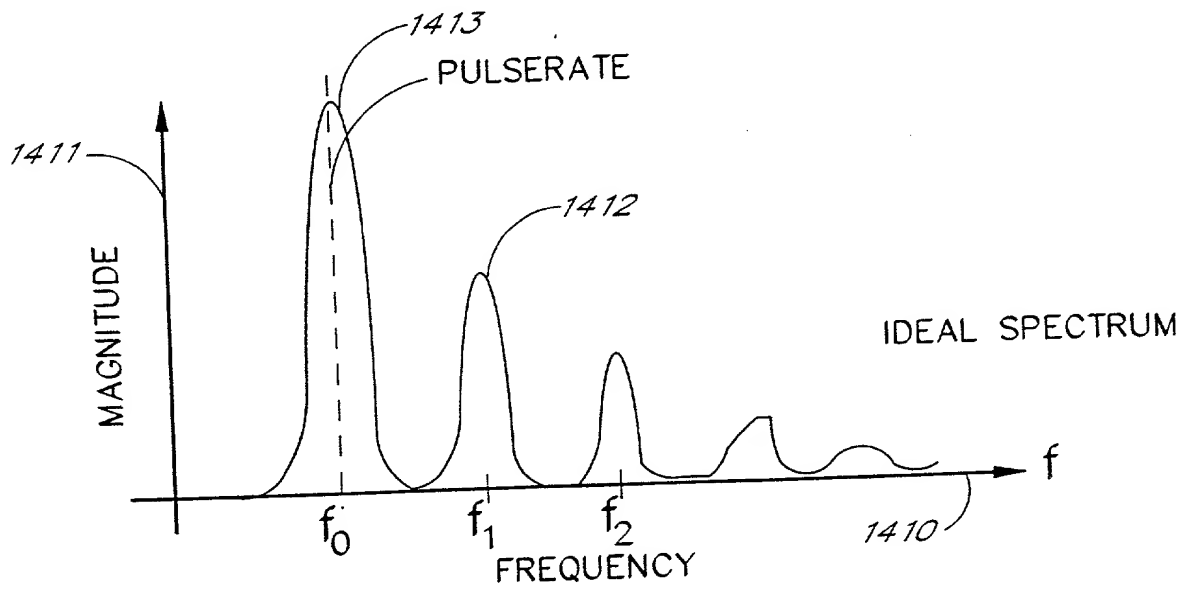


FIG. 14A

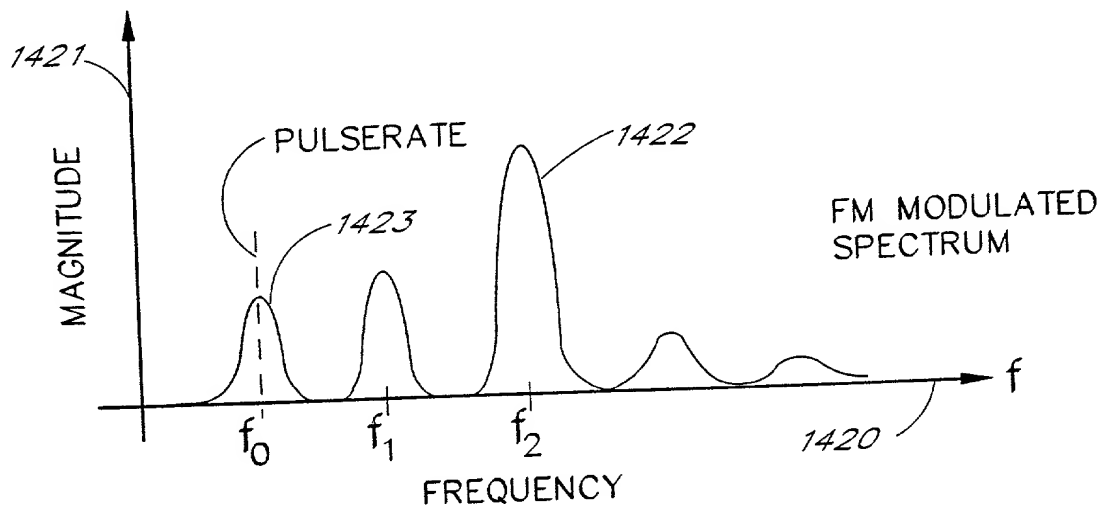


FIG. 14B

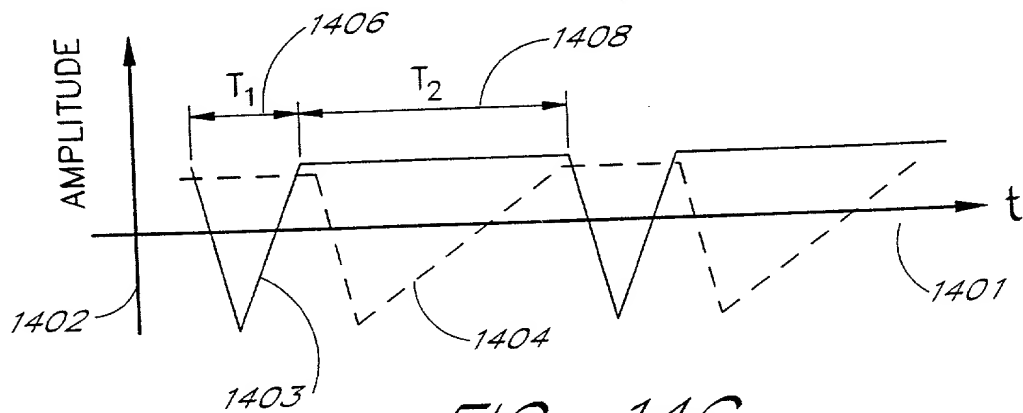


FIG. 14C

AM EFFECTS

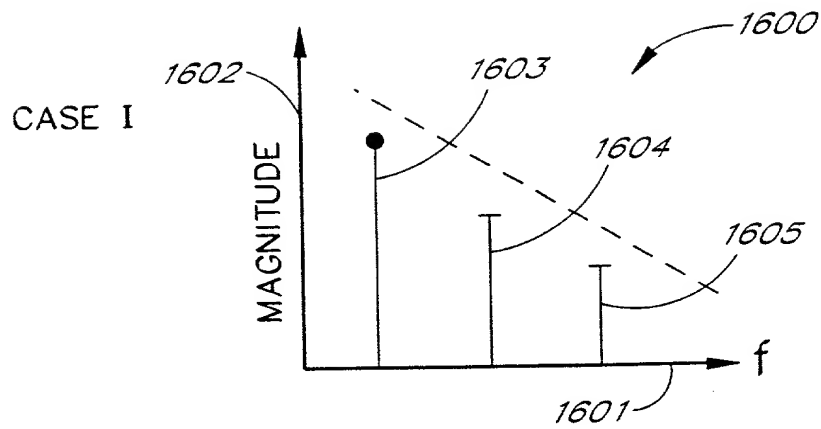


FIG. 16A

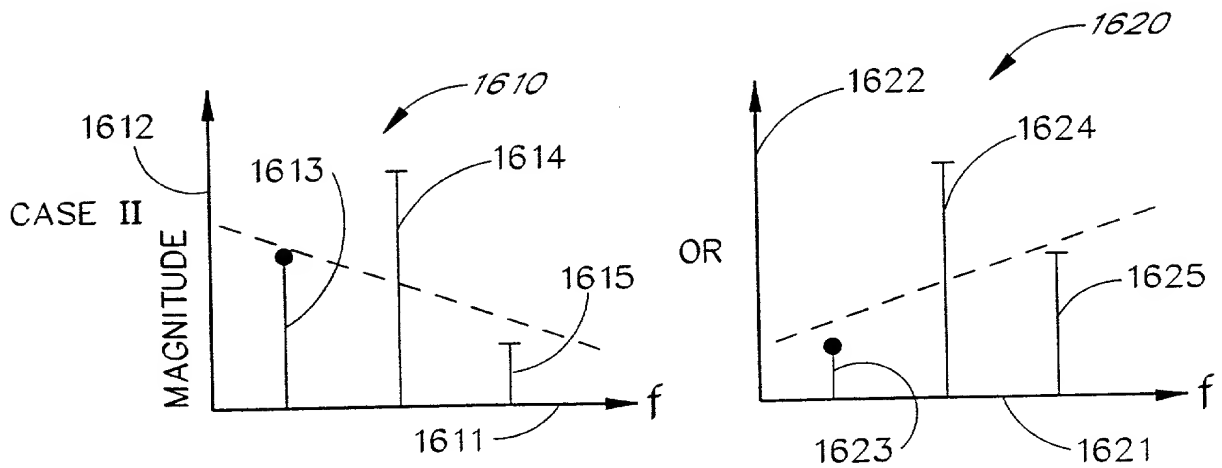


FIG. 16B

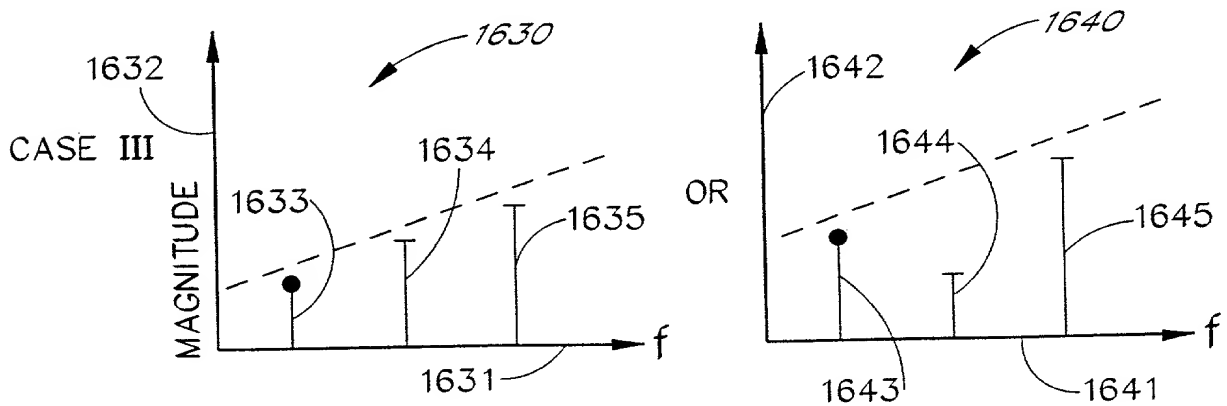


FIG. 16C

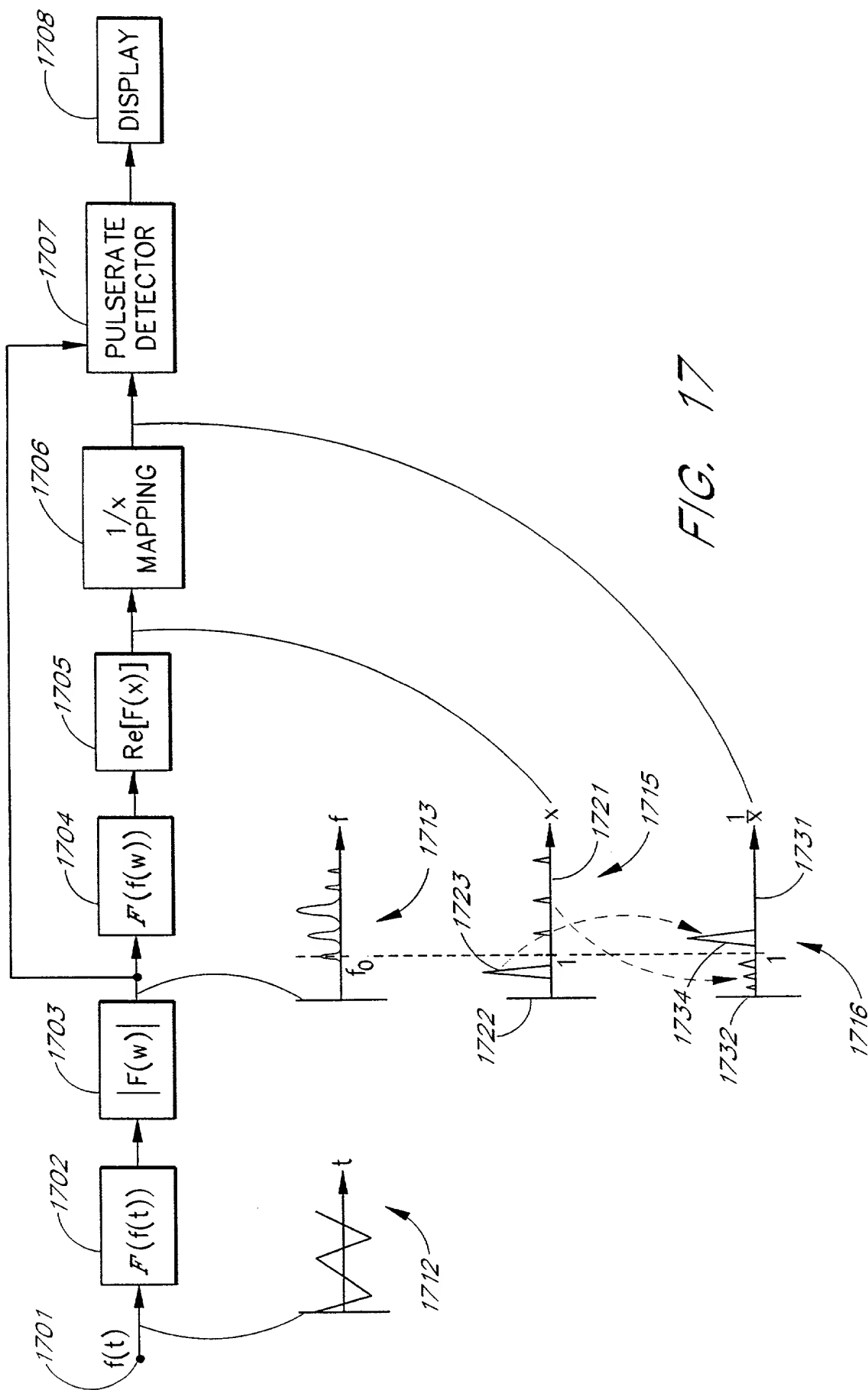


FIG. 17

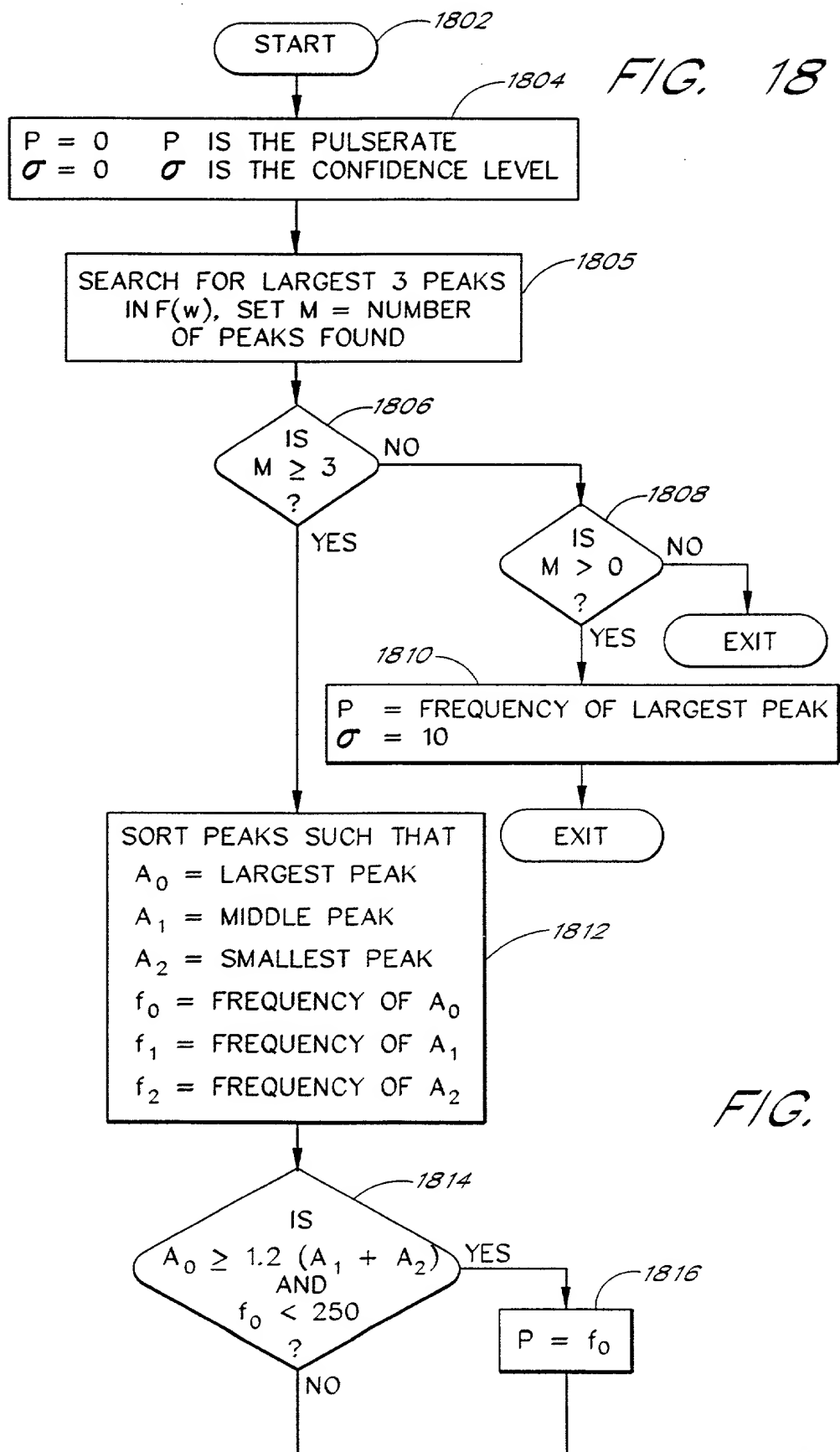
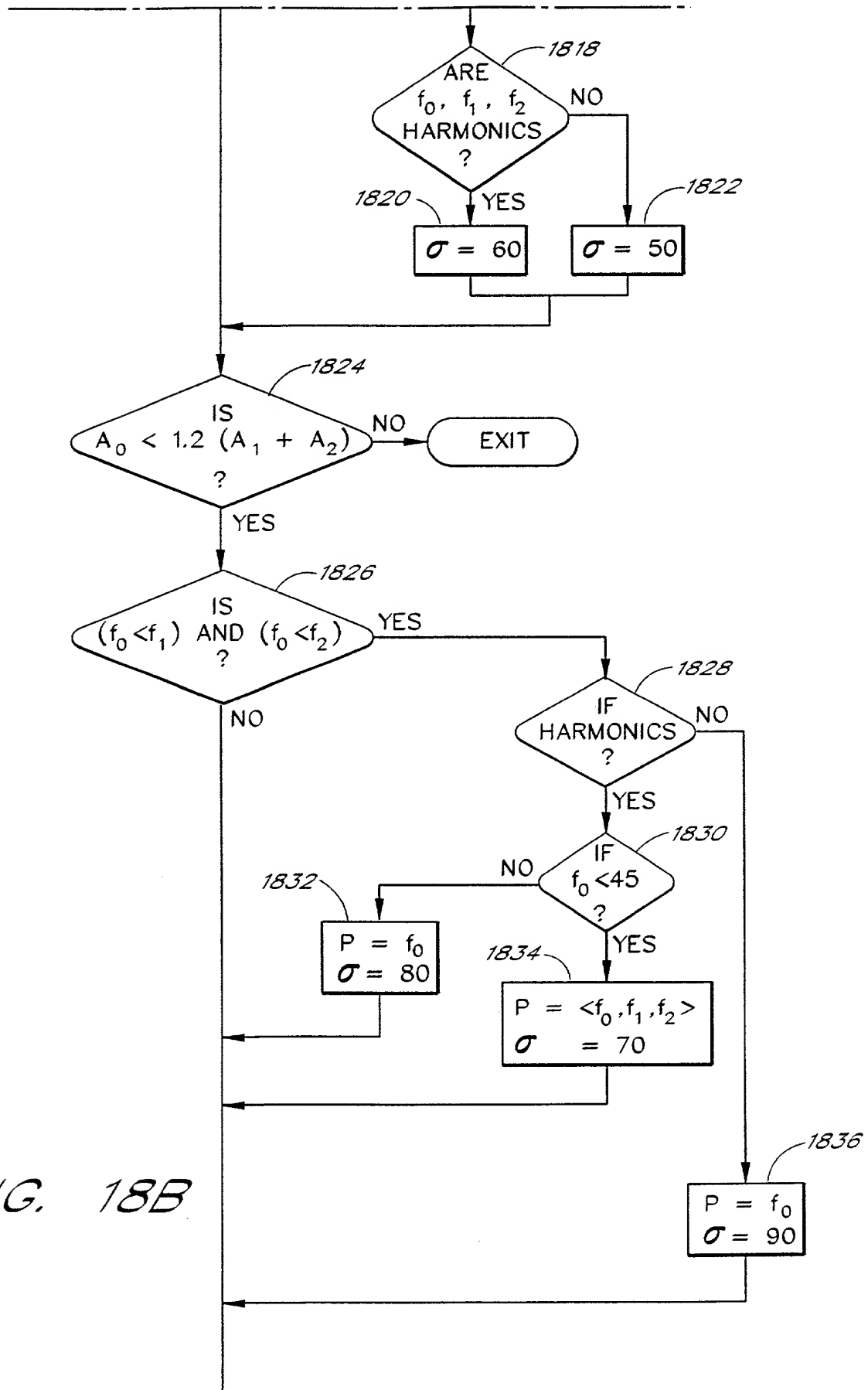


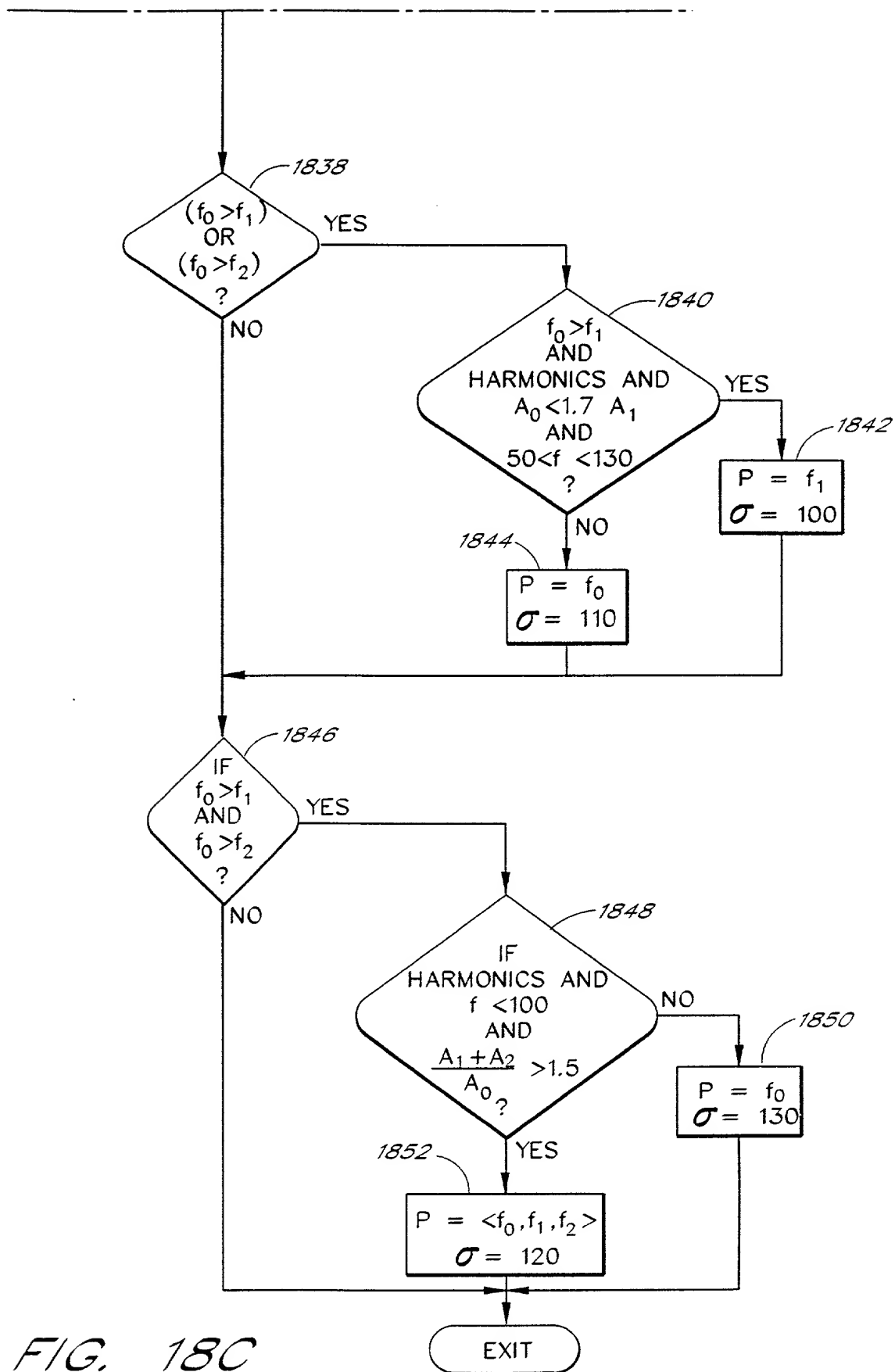
FIG. 18A

FIG. 18B

FIG. 18C

FIG. 18A





DECLARATION - USA PATENT APPLICATION

As a below named inventor, I hereby declare that:

My residence, post office address and citizenship are as stated below next to my name;

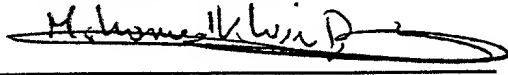
I believe I am an original, first and joint inventor of the subject matter which is claimed and for which a patent is sought on the invention entitled **IMPROVED SIGNAL PROCESSING APPARATUS AND METHOD**; the specification of which is attached hereto;

I hereby state that I have reviewed and understand the contents of the above identified specification, including the claims, as amended by any amendment referred to above;

I acknowledge the duty to disclose information which is material to patentability as defined in Title 37, Code of Federal Regulations, § 1.56;

I hereby declare that all statements made herein of my own knowledge are true and that all statements made on information and belief are believed to be true; and further that these statements were made with the knowledge that willful false statements and the like so made are punishable by fine or imprisonment, or both, under Section 1001 of Title 18 of the United States Code and that such willful, false statements may jeopardize the validity of the application or any patent issued thereon.

Full name of first inventor: **Mohamed K. Diab**

Inventor's signature 

Date 14th of April 1997

Residence: **26945 Diamond, Mission Viejo, California 92691**

Citizenship: **United States**

Post Office Address: **Same as above**

Inventor's signature Per. M. Carthy

Date 14th of April 1997

Post Office Address: Same as above

(714) 760-0404

KNOBBE, MARTENS, OLSON & BEAR, LLP
620 NEWPORT CENTER DR 16TH FLOOR NEWPORT BEACH, CA 92660
(714) 760-0404 FAX (714) 760-9502